Molecular and Cellular Biology

Histone Deacetylases and Phosphorylated Polymerase II C-Terminal Domain Recruit Spt6 for Cotranscriptional Histone Reassembly

Bala Bharathi Burugula, Célia Jeronimo, Rakesh Pathak, Jeffery W. Jones, François Robert and Chhabi K. Govind

Mol. Cell. Biol. **2014, 34(22):4115. DOI: 10.1128/MCB.00695-14.**
Published Ahead of Print 2 September 2014.

MCB
Journals.ASM.org

Histone Deacetylases and Phosphorylated Polymerase II C-Terminal Domain Recruit Spt6 for Cotranscriptional Histone Reassembly

Bala Bharathi Burugula,[a] Célia Jeronimo,[b] Rakesh Pathak,[a] Jeffery W. Jones,[a] François Robert,[b,c] Chhabi K. Govind[a]

Department of Biological Sciences, Oakland University, Rochester, Michigan, USA[a]; Institut de recherches cliniques de Montréal, Montréal, Québec, Canada[b]; Département de Médecine, Faculté de Médecine, Université de Montréal, Montréal, Québec, Canada[c]

Spt6 is a multifunctional histone chaperone involved in the maintenance of chromatin structure during elongation by RNA polymerase II (Pol II). Spt6 has a tandem SH2 (tSH2) domain within its C terminus that recognizes Pol II C-terminal domain (CTD) peptides phosphorylated on Ser2, Ser5, or Try1 *in vitro*. Deleting the tSH2 domain, however, only has a partial effect on Spt6 occupancy *in vivo*, suggesting that more complex mechanisms are involved in the Spt6 recruitment. Our results show that the Ser2 kinases Bur1 and Ctk1, but not the Ser5 kinase Kin28, cooperate in recruiting Spt6, genome-wide. Interestingly, the Ser2 kinases promote the association of Spt6 in early transcribed regions and not toward the 3′ ends of genes, where phosphorylated Ser2 reaches its maximum level. In addition, our results uncover an unexpected role for histone deacetylases (Rpd3 and Hos2) in promoting Spt6 interaction with elongating Pol II. Finally, our data suggest that phosphorylation of the Pol II CTD on Tyr1 promotes the association of Spt6 with the 3′ ends of transcribed genes, independently of Ser2 phosphorylation. Collectively, our results show that a complex network of interactions, involving the Spt6 tSH2 domain, CTD phosphorylation, and histone deacetylases, coordinate the recruitment of Spt6 to transcribed genes *in vivo*.

Dynamic reorganization of chromatin structure is important for the regulation of transcription by RNA polymerase II (Pol II). Several ATP-dependent chromatin remodelers, histone-modifying enzymes, and histone chaperones promote the disruption of chromatin structure to allow transcription by Pol II and to restore chromatin structure in the wake of transcription (1, 2). Spt6 is a highly conserved and multifunctional protein shown to regulate multiple steps of transcription, including initiation (3, 4) and elongation (5, 6). In addition, it is important for other DNA-dependent processes such as recombination (7, 8), mRNA export (9), and viral replication (10).

Spt6 interacts with histones H3 and H4 (11) and functions as a histone chaperone to regulate cotranscriptional nucleosome reassembly and to modulate chromatin structure, including histone modifications (11–15). Depletion of Spt6 in yeast (*Saccharomyces cerevisiae*) causes a widespread reduction in histone H3 primarily from the 5′ ends of transcribed genes, indicating the importance of Spt6 in maintaining histone occupancy (16). One of the effects of losing Spt6 function is altered gene expression and activation of intragenic cryptic transcription (17–19). Aberrant transcription is also associated with histone deacetylase (HDAC) mutants. Impairing the function of the HDAC Rpd3-small (Rpd3S) and Hos2-Set3 complexes leads to cryptic and antisense transcription genome-wide (20, 21). It is not clear whether Spt6 and HDACs collaborate to suppress spurious transcription.

Spt6 localization to transcribed regions strongly correlates with Pol II occupancy (15, 22). It possesses a tandem Src homology 2 domain (tSH2) that interacts with phosphorylated Pol II C-terminal domain (CTD) peptides *in vitro* and is required for full recruitment of Spt6 *in vivo* (22–26). Although these observations suggest that CTD phosphorylation is needed for Spt6 recruitment, the role of CTD phosphorylation *in vivo* in this process is not fully understood. Notably, while the two phosphorylated CTD residues implicated in Spt6 recruitment, Ser2 and Tyr1, peak near the 3′ ends of transcribed genes, Spt6 recruitment begins slightly downstream of the transcription start site (TSS) (22, 23). Moreover, deletion of the primary Ser2 CTD kinase *CTK1* does not affect Spt6 recruitment *in vivo* (27). To account for these observations, it has been suggested that initial recruitment of Spt6 near TSS occurs in a Ser2 phosphorylation-independent manner. It is therefore not evident whether Ser2 or Try1 phosphorylation is important for Spt6 recruitment *in vivo* and whether they cooperate or function independently in this process. In order to resolve these inconsistencies in the role of CTD phosphorylation in Spt6 recruitment, we systematically analyzed its genome-wide occupancy in Pol II CTD kinase mutants.

We report here that Ser2 kinases Bur1 and Ctk1, but not the Ser5 kinase Kin28, cooperate to recruit Spt6 near the TSS. Interestingly, we show that HDACs are required to maintain high Spt6 occupancy across the transcribed region by stabilizing Spt6 interaction with phosphorylated Pol II. This function in stimulating Spt6 recruitment by HDACs in the coding regions is independent of methylation-dependent histone deacetylation. Furthermore, our data suggest that recruitment of Spt6 near 3′ regions of transcribed genes is promoted by Tyr1 phosphorylation in a manner independent of Ser2/Ser5 kinases. We therefore propose that CTD serine kinases and HDACs coordinate the recruitment of Spt6 to the transcribed region. In

Received 22 May 2014 Returned for modification 16 June 2014
Accepted 25 August 2014
Published ahead of print 2 September 2014
Address correspondence to Chhabi K. Govind, govind@oakland.edu.
Supplemental material for this article may be found at http://dx.doi.org/10.1128/MCB.00695-14.

doi:10.1128/MCB.00695-14

TABLE 1 Yeast strains used in this study

Strain	Parent	Genotype	Source or reference
Untagged strains			
BBY 1205 (WT Ser5 kinases)	S288C	*MATα ade2::hisG his3Δ200 leu2Δ0 lys2Δ0 met15Δ0 trp1Δ63 ura3Δ0*	29
BBY 1207 (*kin28as/bur2Δ*)	S288C	*MATα ade2::hisG his3Δ200 leu2Δ0 lys2Δ0 met15Δ0 trp1Δ63 ura3Δ0 kin28::kin28-L83G Δbur2::Leu2* [pSH579 *ARS CEN URA3 kin28-L83G*]	29
BBY 1107 (WT Ser2 kinases)	BY 4741	*MAT***a** *his3Δ1 leu2Δ0 met15Δ0 ura3Δ0*	28
BBY 1110 (*bur1as/ctk1Δ*)	BY 4741	*MAT***a** *his3Δ1 leu2Δ0 met15Δ0 ura3Δ0 bur1as ctk1Δ::kanMX4*	28
BBY 1103 (WT HDACs)	BY 4705	*MATα ade2Δ::hisG HIS3Δ200 LEU2Δ0 ura3Δ0 trp1Δ63 LYS2Δ0 met15Δ0*	30
BBY 1104 (*rpd3Δ/hos2Δ*)	BY 4705	*MATα ade2Δ::hisG HIS3Δ200 LEU2Δ0 ura3Δ0 trp1Δ63 LYS2Δ0 met15Δ0 rpd3::LEU2 hos2::LYS2*	30
BBY 1213	1257	*MAT***a** *his3Δ1 leu2Δ0 met15Δ0 ura3Δ0 set1Δ::hphMX4 set2Δ::kanMX4*	31
BBY 1211	BY 4741	*MAT***a** *his3Δ1 leu2Δ0 met15Δ0 ura3Δ0 set1Δ::hphMX4*	31
BBY 1212	BY 4741	*MAT***a** *his3Δ1 leu2Δ0 met15Δ0 ura3Δ0 set2Δ::kanMX4*	31
BBY 1101	R1158	*pSPT6::kanR-tet07-TATA URA3::CMV-tTA MAT***a** *his3Δ1 leu2Δ0 met15Δ0*	Thermo Scientific
BBY 1130 (WT H3)	S288C	*MAT***a** *his3Δ200 leu2Δ0 lys2Δ0 trp1Δ63 ura3Δ0 met15Δ0 can1::MFA1pr-HIS3 hht1-hhf1::NatMX4 hht2-hhf2::*[*HHTS-HHFS*]*-URA3*	Thermo Scientific
BBY 1140 (WT H4)	S288C	*MAT***a** *his3Δ200 leu2Δ0 lys2Δ0 trp1Δ63 ura3Δ0 met15Δ0 can1::MFA1pr-HIS3 hht1-hhf1::NatMX4 hht2-hhf2::*[*HHTS-HHFS*]*-URA3*	Thermo Scientific
Myc-tagged strains			
BBY 1208	S288C	*MATα ade2::hisG his3Δ200 leu2Δ 0 lys2Δ0 met15Δ0 trp1Δ63 ura3Δ0 SPT6-13myc::HIS3*	This study
BBY 1210	S288C	*MATα ade2::hisG his3Δ200 leu2Δ0 lys2Δ0 met15Δ0 trp1Δ63 ura3Δ0 kin28::kin28-L83G Δbur2::Leu2* [pSH579 *ARS CEN URA3 kin28-L83G*] *SPT6-13myc::HIS3*	This study
BBY 1209	S288C	*MATα ade2::hisG his3Δ200 leu2Δ0 lys2Δ0 met15Δ0 trp1Δ63 ura3Δ0 kin28::kin28-L83G* [pSH579 *ARS CEN URA3 kin28-L83c*]*SPT6-13myc::HIS3*	This study
BBY 1111	BY 4741	*MAT***a** *his3Δ1 leu2Δ0 met15Δ0 ura3Δ0 SPT6-13myc::HIS3*	This study
BBY 1112	BY 4741	*MAT***a** *his3Δ1 leu2Δ0 met15Δ0 ura3Δ0 bur1as SPT6-13myc::HIS3*	This study
BBY 1113	BY 4741	*MAT***a** *his3Δ1 leu2Δ0 met15Δ0 ura3Δ0 ctk1Δ::kanMX4 SPT6-13myc::HIS3*	This study
BBY 1114	BY 4741	*MAT***a** *his3Δ1 leu2Δ0 met15Δ0 ura3Δ0 bur1as ctk1Δ::kanMX4 SPT6-13myc::HIS3*	This study
BBY 1105	BY 4705	*MATα ade2Δ::hisG HIS3Δ200 LEU2Δ0 ura3Δ0 trp1Δ63 LYS2Δ0 met15Δ0 SPT6-13myc::HIS3*	This study
BBY 1106	BY 4705	*MATα ade2Δ::hisG HIS3Δ200 LEU2Δ0 ura3Δ0 trp1Δ63 LYS2Δ0 met15Δ0 rpd3::LEU2 hos2::LYS2 SPT6-13myc::HIS3*	This study
BBY 1218	1257	*MAT***a** *his3Δ1 leu2Δ0 met15Δ0 ura3Δ0 set1Δ::hphMX4 set2Δ::kanMX4 SPT6-13myc::HIS3*	This study
BBY 1216	BY4741	*MAT***a** *his3Δ1 leu2Δ0 met15Δ0 ura3Δ0 set1Δ::hphMX4 SPT6-13myc::HIS3*	This study
BBY 1217	BY4741	*MAT***a** *his3Δ1 leu2Δ0 met15Δ0 ura3Δ0 set2Δ::kanMX4 SPT6-13myc::HIS3*	This study
BBY 1102	R1158	*pSPT6::kanR-tet07-TATA URA3::CMV-tTA MAT***a** *his3Δ1 leu2Δ0 met15Δ0 SPT6-13myc::HIS3*	This study
BBY 1131 (H3 K4, K9, K14, K18-A)	S288C	*MAT***a** *his3Δ200 leu2Δ0 lys2Δ0 trp1Δ63 ura3Δ0 met15Δ0 can1::MFA1pr-HIS3 hht1-hhf1::NatMX4 hht2-hhf2::*[*hhts* K4,9,14,18A-*HHFS*]*-URA3 SPT6-13myc::HIS3*	This study
BBY 1132 (H3 Δ1-28)	S288C	*MAT***a** *his3Δ200 leu2Δ0 lys2Δ0 trp1Δ63 ura3Δ0 met15Δ0 can1::MFA1pr-HIS3 hht1-hhf1::NatMX4 hht2-hhf2::*[*hhts* (Δ1-28)*-HHFS*]*-URA3 SPT6-13myc::HIS3*	This study
BBY 1141 (H4 Δ1-16)	S288C	*MAT***a** *his3Δ200 leu2Δ0 lys2Δ0 trp1Δ63 ura3Δ0 met15Δ0 can1::MFA1pr-HIS3 hht1-hhf1::NatMX4 hht2-hhf2::*[*HHTS-hhfs* (Δ1-16)]*-URA3 SPT6-13myc::HIS3*	This study
BBY 1142 (H4 Δ1-24)	S288C	*MAT***a** *his3Δ200 leu2Δ0 lys2Δ0 trp1Δ63 ura3Δ0 met15Δ0 can1::MFA1pr-HIS3 hht1-hhf1::NatMX4 hht2-hhf2::*[*HHTS-hhfs* (Δ1-24)]*-URA3 SPT6-13myc::HIS3*	This study
spt6Δ202-Myc-tagged strains			
BBY 1219	BY4705	*MATα ade2Δ::hisG HIS3Δ200 LEU2Δ0 ura3Δ0 trp1Δ63 LYS2Δ0 met15Δ0 SPT6Δ202-13myc::HIS3*	This study
BBY 1220	BY4705	*MATα ade2Δ::hisG HIS3Δ200 LEU2Δ0 ura3Δ0 trp1Δ63 LYS2Δ0 met15Δ0 rpd3::LEU2 hos2::LYS2 SPT6Δ202-13myc::HIS3*	This study

addition, our data show that the recruitment of Spt6 at the very 3′ end of a transcribed gene is tSH2 mediated and Ser2 phosphorylation (Ser2P) independent, possibly occurring through CTD-Tyr1 phosphorylation.

MATERIALS AND METHODS

Yeast strains. All of the yeast strains used in the present study are listed in Table 1. The wild-type (WT) BY4741 and deletion derivatives (32), including *SPT6-tet* (33), were purchased from Thermo Scientific,

TABLE 2 Sequences of the primers used in this study

Primer sequence (5′–3′)	Gene and location[a]
GACAAAATGAAGAAAATGCTGATGCACC	*POL1* ORF (F)
TAATAACCTTGGTAAAACACCCTG	*POL1* ORF (R)
GCTGAGTTTAACGGTGATTATT	*TEL VI-R* (F)
CCAGTCCTCATTTCCATCAAT	*TEL VI-R* (R)
ACGGCTCTCCAGTCATTTAT	*ARG1* UAS (F)
GCAGTCATCAATCTGATCCA	*ARG1* UAS (R)
TAATCTGAGCAGTTGCGAGA	*ARG1* TATA (F)
ATGTTCCTTATCGCTGCACA	*ARG1* TATA (R)
TGGCTTATTCTGGTGGTTTAG	*ARG1* 5′ORF (F)
ATCCACACAAACGAACTTGCA	*ARG1* 5′ORF (R)
TTCTGGGCAGATCTACAAAGA	*ARG1* 3′ORF (F)
AAGTCAACTCTTCACCTTTGG	*ARG1* 3′ORF (R)
TATACGGCCTTCCTTCCAGTT	*ADH1* CORE (F)
TGTGCAGCAAAAGAAACAAGGA	*ADH1* CORE (R)
CCCACGGTAAGTTGGAATACA	*ADH1* 5′ORF (F)
TGACCACCGACTAATGGTAGC	*ADH1* 5′ORF (R)
CTTACGTCGGTAACAGAGCTGA	*ADH1* 3′ORF (F)
ACCAACGATTTGACCCTTTTC	*ADH1* 3′ORF (R)
CGACGACGAAGACAGTGATA	*PMA1* 5′ORF (F)
ATTCTTTTTCGTCAGCCATTG	*PMA1* 5′ORF (R)
TGTTTTGGGTGGTTTCTACTACG	*PMA1* 3′ORF (F)
TTAGGTTTCCTTTTCGTGTTAGAG	*PMA1* 3′ORF (R)
AAATAGGCACAAACACGACC	*STE11* 3′ORF (F)
ATTATGTGTGCATCCAGCCA	*STE11* 3′ORF (R)
GCTGATGAAACCTCTGCATCTAC	*FLO8* 3′ORF (F)
CAACCATACCAATATTCCCAA	*FLO8* 3′ORF (R)
GAAACAAGAACTGGAAGATGCCGAAGAGGAGAGG AAATTGATGATGGCAGAAGCCCGTGCAAAG AGACGGATCCCCGGGTTAATTAA	*SPT6Δ202*-Myc tagging (F)
TTTGTAATGGTTTTAAGACGCTTCTAAAATCT AACAGTAGTAAGAATAGAATGAACAACTA CCGTCGGATCCCCGGGTTAATTAA	Spt6-Myc tagging (F)
CTTACCTAAACAATGGTCAAAGTAATAATAAA ATTAATAATAACAATGGACACTACATACG CATGAATTCGAGCTCGTTTAAAC	Spt6-Myc tagging (R)

[a] F and R, forward and reverse primer sequences, respectively.

USA. Myc-tagged strains were generated as described previously (34). Briefly, plasmid pFA6a-13Myc-His3MX6 was used as a template to PCR amplify using primers with flanking nucleotides homologous to upstream and downstream regions of the stop codon of Spt6. The last 202 amino acid residues of Spt6 were deleted by inserting 13Myc at residue 1250 of Spt6 to generate the *spt6Δ202*-Myc-tagged strain. The primers used are listed in Table 2.

Growth conditions. For chromatin immunoprecipitation, saturated overnight cultures were subcultured in 100 ml of synthetic complete (SC) medium lacking isoleucine/valine and were grown to an A_{600} of between 0.5 and 0.6. The cultures were treated with 0.65 μg of sulfometuron methyl (SM)/ml for 25 min to induce Gcn4. Analog-sensitive Ser2 kinase mutants (*bur1as* and *bur1as*/*ctk1*Δ) were treated with 6 μM 3MB-PP1 1 h prior to the addition of SM, as described previously (28). Similarly, Ser5 kinase mutants (*kin28as* and *kin28as*/*bur2*Δ) were treated with 6 μM NA-PP1 for 15 min prior to Gcn4 induction by SM, as described previously (29, 35). *SPT6-tet* cells (Thermo Scientific) were grown in the media containing 10 μg of doxycycline to deplete Spt6 (33). For coimmunoprecipitation experiments, the cells were grown in yeast extract-peptone-dextrose (YPD) medium to an A_{600} of 2 to 3.

Western blot analysis. Western blot analysis was carried out by either using a fraction of cells collected for chromatin preparation as described above or growing cells overnight in 5 ml of synthetic complete media. Whole-cell extracts (WCE) were prepared by the trichloroacetic acid (TCA) precipitation method (35). Briefly, the cell pellets were disrupted by using glass beads in the presence of 20% TCA, and the cell extracts were collected. The beads were washed once with 5% TCA, and the extracts thus obtained were pooled with the cell extracts collected upon 20% TCA extraction. The extracts were centrifuged, and the pellet was resuspended in 50 to 100 μl of 1 M Tris buffer (pH 8.0) to neutralize the pH. An equal volume of 2× sodium dodecyl sulfate (SDS) sample buffer was added to the extracts, and the proteins were separated on 8% SDS-polyacrylamide gels and transferred to a nitrocellulose membrane. The membranes were probed with the indicated antibodies, and signals were detected by enhanced chemiluminescence (ECL; GE Healthcare, catalog no. RPN2106). The signals were quantified using Image Studio Lite (LI-COR Biosciences).

ChIP experiments. Chromatin immunoprecipitation (ChIP) experiments were performed as described previously (36). Briefly, 100 ml of cells (A_{600} = 0.6) were cross-linked with 1% formaldehyde for 15 min at ambient temperature and quenched with glycine. Chromatin was isolated and fragmented by sonication (Branson 450) to an average size of 300 to 400 bp. The soluble fraction of chromatin was used for ChIP using antibodies against Myc (Roche; catalog no. 11667203001), Rpb3 (Neoclone; W0012), histone H3 (Abcam; ab1791), acetylated H3 (Millipore; 06-599), acetylated H4 (Millipore; catalog no. 06-866), phosphorylated Ser5 (Covance; MMS-134R), and phosphorylated Ser2 (Bethyl Laboratories; A300-654A). The primers used to amplify specific regions of *ARG1*, *ADH1*, and *PMA1* and the internal control *POL1* are listed in Table 2. SYBR green dye was added to the PCR-amplified DNA, resolved on 8% Tris-borate-EDTA gels, and the signals were quantified by using a phosphorimager. Fold enrichments (ChIP/inputs) were determined by normalizing the specific region/*POL1* ChIP ratios to the ratios obtained for the input samples. For histone acetylation ChIPs, a region of the right arm of *TEL VI* was used as an internal control instead of *POL1*. The acetylhistone/*TEL VI* ratio was further normalized to the H3 occupancy/*POL1* in order to account for the changes in nucleosome density in the histone methyltransferase mutants. The data represent the average of ChIP performed using the chromatin prepared from at least three independent cultures, and PCRs were performed in duplicate for each ChIP sample.

ChIP-chip experiments. ChIP experiments were performed as described above, and ChIP DNA was hybridized on tiling microarrays, custom designed by Agilent Technologies and contain a total of about 180,000 melting temperature (T_m)-adjusted 60-mer probes covering the entire yeast genome with virtually no gaps between probes. Spt6-Myc ChIP samples were hybridized in competition with control ChIP DNAs prepared from an isogenic untagged strain, except in Fig. 6, where Spt6 ChIP DNA was hybridized in competition with input DNA. Rpb3 ChIP DNA was hybridized in competition with input DNA. ChIP with microarray technology (ChIP-chip) data were normalized using the Limma Loess method, and replicates (at least duplicates) were combined as described previously (37).

Aggregate profiles. Aggregate profiles were generated using the versatile aggregate profiler (38). In brief, genes were virtually cut in the middle and the first half aligned on the TSS, while the second half was aligned on the poly(A) (pA) site. The TSS and pA sites were deduced using the untranslated region (UTR) sizes as determined by Xu et al. (39). Genes for which the 5′ and 3′ UTRs have not been previously determined were therefore not included in these analyses. The aligned data were averaged over 50-bp bins (10 bins upstream from the TSS, 40 bins downstream from the TSS, and 10 bins downstream of the pA). The genes included in each specific analysis are described in the figure legends.

The normalized $\log_2$ enrichment values in the coding region were averaged to obtained open reading frame (ORF) enrichment for Spt6 and Rpb3. The top 25% of genes (n = 1,580) bound by Spt6 were selected and analyzed. Similarly, Rpb3 ORF values were determined and used to plot Spt6 occupancy based on the average Pol II occupancy observed in the isogenic WT strain.

Coimmunoprecipitation experiments. Coimmunoprecipitation experiments were performed as described previously (35). Cells were grown in YPD to an A_{600} of 2.0, and the whole-cell extracts (0.5 to 1 mg) were lysed in lysis buffer [50 mM Tris-HCl (pH 7.5), 50 mM HEPES-KOH (pH 7.9), 10 mM $MgSO_4$, 100 mM $(NH_4)_2SO_4$, 12.5 mM potassium acetate, 0.01% NP-40, 20% glycerol, 1 μg/ml pepstatin A, 100 mM phenylmethylsulfonyl fluoride [PMSF], 1 μg/ml leupeptin]. Whole-cell extracts thus prepared were incubated with magnetic bead-conjugated anti-Myc antibodies in 1× MTB buffer (4× MTB buffer is 200 mM HEPES-KOH [pH 7.9], 800 mM potassium acetate, 54 mM magnesium acetate, 40% glycerol, 0.04% NP-40, 400 mM PMSF, 4 μg/ml pepstatin, 4 μg/ml leupeptin) for 2 h and washed three times with wash buffer (50 mM Tris-HCl [pH 8.0], 0.1% NP-40, 150 mM NaCl, 10% glycerol, 1 mM PMSF, 1 μg/ml leupeptin, 1 μg/ml pepstatin, and phosphatase inhibitors [Sigma; catalog no. P0044]). The immunoprecipitates were processed for Western blot analysis. The experiments were performed using at least three independent cultures.

Peptide pulldown assay. WCEs (0.5 to 1 mg) were incubated with 5 μg of biotinylated histone tail peptides purchased from Anaspec, USA (H3, catalog no. 61702; acetylated H3, catalog no. 65277; H4, catalog no. 65242, and acetylated H4, catalog no. 65248) overnight at 4°C. Streptavidin beads were preincubated with phosphate-buffered saline–bovine serum albumin (5%) for 1 h, washed once with 500 μl of high-salt wash buffer (25 mM Tris-HCl [pH 8.0], 1 M NaCl, 1 mM dithiothreitol [DTT], 5% glycerol, 003% NP-40), and washed twice with 500 μl of binding buffer (25 mM Tris-HCl [pH 8.0], 500 mM NaCl, 1 mM DTT, 5% glycerol, 0.03% NP-40). The mixture of peptide and WCEs was added to the pretreated streptavidin beads, incubated for 3 h, and washed with wash buffer containing 150 mM NaCl to collect peptide-protein complexes. The presence of Spt6 in the pulldown was detected by Western blotting. These experiments were repeated three times with reproducible results.

RESULTS

Ser2 kinases recruit Spt6 to coding regions. To investigate the mechanisms of Spt6 recruitment, we used *ARG1*, a Gcn4 target gene, which is induced under amino acid starvation conditions. *ARG1* was induced by treating cells with sulfometuron methyl (SM), an inhibitor of isoleucine-valine biosynthesis, and the Pol II (Rpb3) and Myc-tagged Spt6 (Spt6-Myc) occupancies were determined by chromatin immunoprecipitation (ChIP). In agreement with previous studies (15, 22), SM treatment increased Rpb3 (Pol II subunit) binding to both promoter and coding regions of the *ARG1* gene and increased Spt6-Myc binding primarily to the *ARG1* coding region (data not shown).

To determine the role of Pol II CTD phosphorylation in recruiting Spt6, we first analyzed its occupancy in the Ser2 CTD kinase mutants, *ctk1*Δ, *bur1as* (as, analog sensitive), and *bur1as/ctk1*Δ by ChIP at the *ARG1* gene. The kinase activity of *bur1as* is rapidly inhibited by treating growing cells with the ATP analog 3MB-PP1 prior to induction by SM (28). As expected, the Ser2P levels were higher in the *ARG1* 3′ part of the coding region (here called the 3′ORF) than in the 5′ part of the coding region (here called the 5′ORF) in WT cells (Fig. 1A) and were substantially reduced across the *ARG1* coding region in the *ctk1*Δ and *bur1as/ctk1*Δ mutants. This is consistent with the fact that Ctk1 is responsible for the majority of Ser2 phosphorylation *in vivo* (40, 41). The *bur1as* mutant treated with 3MB-PP1 reduced Ser2P only in the 5′ORF. This last result is in agreement with the role of Bur1 in phosphorylating Ser2 at promoter-proximal regions (28, 42). In contrast to the large reduction in Ser2P in the *ctk1*Δ mutant, Spt6 binding was only modestly reduced at the *ARG1* ORF in this mutant (Fig. 1B). Similarly, a reduction in Spt6 binding was also observed in the *bur1as* mutant in the *ARG1* 5′ORF and, interestingly, greater reductions in the *ARG1* 5′ORF and 3′ORF were observed in the *bur1as/ctk1*Δ mutant. We, however, noted that total Pol II occupancy over the *ARG1* coding region was reduced in *ctk1*Δ and *bur1as/ctk1*Δ cells (Fig. 1C). To account for this effect, we calculated the Spt6-Myc/Rpb3 ratio in WT and kinase mutants and found that the Spt6-Myc/Rpb3 ratios were similar in the WT and *ctk1*Δ cells, indicating that Ctk1 is dispensable for Spt6 recruitment (Fig. 1D), an observation in agreement with a previous report (27). A greater reduction in the Spt6-Myc/Rpb3 ratio at both the 5′ORF and the 3′ORF of the *ARG1* gene was observed in the *bur1as/ctk1*Δ mutant compared to the *bur1as* mutant (Fig. 1D), indicating that both Bur1 and Ctk1 contribute to the full recruitment of Spt6 *in vivo*. Similarly, at the *ADH1* gene, a greater Spt6 binding defect was observed in the double mutant than in the respective single mutants (Fig. 1E).

A recent study suggested that the deletion of *CTK1* greatly reduces Spt6 cellular levels (43). Although *ctk1*Δ did not reduce Spt6 occupancy in the coding regions in our experiments (Fig. 1B and 1D) (27), we nonetheless determined Spt6 levels in the Ser2 kinases mutants. The Spt6 protein levels were largely unaffected in *ctk1*Δ, *bur1as*, or *bur1as/ctk1*Δ cells (Fig. 1F). Similarly, no reduction in Spt6 levels was observed in chromatin samples used for ChIP analysis or in cells grown in YPD medium (data not shown). Nearly equal levels of Spt6 were also observed in untagged strains, ruling out the possibility that introducing the Myc tag stabilized the protein in the *ctk1*Δ mutant (Fig. 1G). The discrepancy between our results regarding the levels of Spt6 in the *ctk1*Δ mutant and those obtained by a previous study (43) might indicate the differences in whole-cell extract preparation and preservation of protein stability. Altogether, our results (Fig. 1A to E) suggest that Ser2 phosphorylation by both Bur1 and Ctk1 contribute to Spt6 recruitment in the coding regions.

Ser2 kinases promote Spt6 recruitment to the 5′ coding regions genome-wide. In order to look at the possible contribution of Ser2 phosphorylation on Spt6 recruitment at a global scale, we made use of *bur1as/ctk1*Δ cells. The *bur1as/ctk1*Δ cells were treated with 3MB-PP1 to inactivate the Bur1 kinase activity, and Rpb3 and Spt6-Myc immunoprecipitated DNA were hybridized on 4x180K Agilent arrays (see Materials and Methods) to determine their genome-wide occupancy.

In agreement with previous studies (15, 22), the average Spt6 occupancy in the coding regions very strongly correlated with Rpb3 occupancy in WT cells (Fig. 2A) ($r = 0.91$, Pearson correlation; see also Table S1 in the supplemental material). To examine whether Spt6 occupancy is affected in *bur1as/ctk1*Δ cells, we selected the top 25% of the Spt6-occupied genes, based on the average Spt6 occupancy over each transcribed region ($n = 1{,}580$; see Table S1 in the supplemental material) and plotted the average Rpb3 and Spt6 $\log_2$ values for these genes. Although the Rpb3 occupancy in the mutant strongly correlated (Fig. 2B) ($r = 0.85$, Pearson) with that of WT cells at the top 25% of Spt6 occupied genes, only a moderate correlation ($r = 0.57$) was observed between Spt6 occupancy in the mutants and Rpb3 in WT cells. This suggests that Ser2 kinases are important for recruiting Spt6 (Fig. 2B). More importantly, in the *bur1as/ctk1*Δ mutant, Spt6 binding was primarily reduced at the 5′ ends of genes, with only minor defects in the 3′ORF (Fig. 2C). This was somewhat surprising given that Ser2 phosphorylation is primarily detected nearing the 3′ORF. This result suggests that phosphorylation of few (perhaps

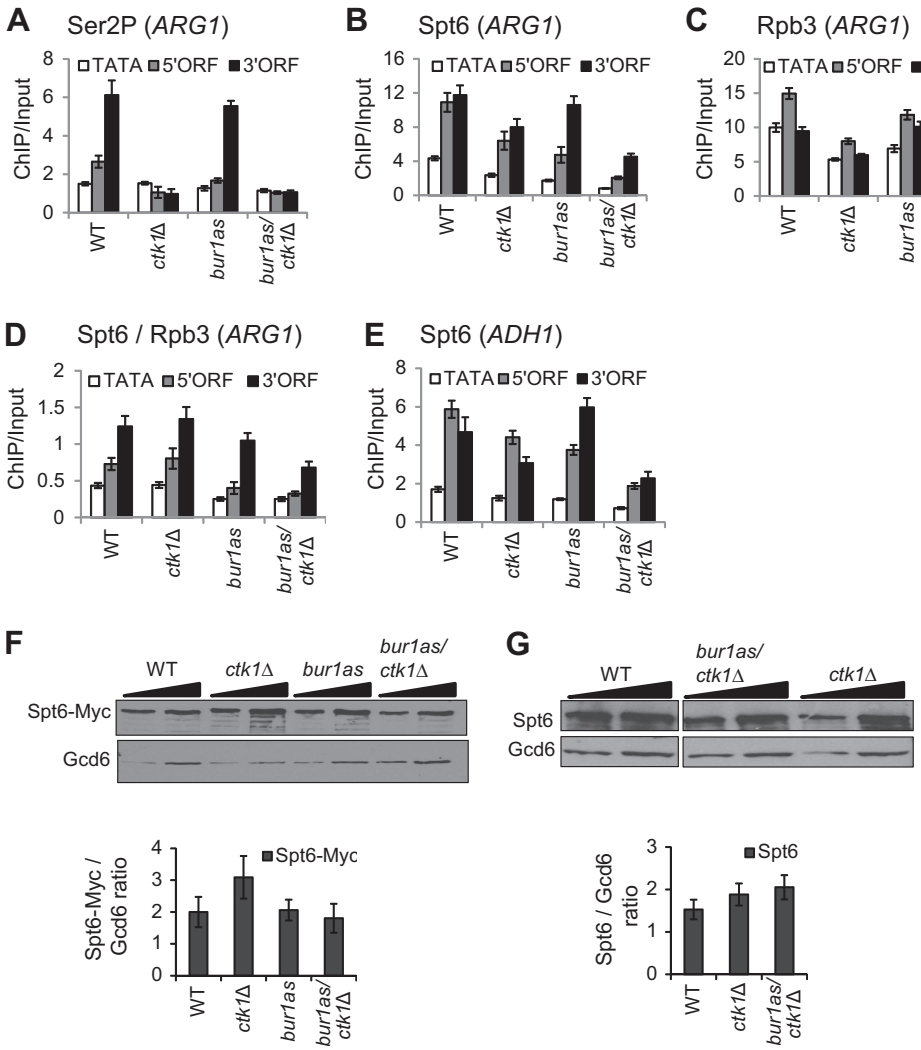

FIG 1 Ser2 kinases promote Spt6 recruitment to coding regions. (A to E) WT, *ctk1*Δ, *bur1as*, and *bur1as*/*ctk1*Δ cells expressing Myc-tagged Spt6 were treated with a 6 μM concentration of ATP analog (3MB-PP1) to inhibit Bur1 kinase activity for 1 h prior to the induction of Gcn4 target genes by SM for additional 25 min. Chromatin extracts were subjected to ChIP using antibodies against serine2 phosphorylated Pol II (Ser2P), Myc, or Rpb3. ChIP occupancy of Ser2P (A), Spt6-Myc (B), and total Pol II (Rpb3) (C) at the promoter (TATA), as well as the 5′ (5′ORF) and the 3′ parts (3′ORF) of the *ARG1* coding region, is shown. (D) Spt6-Myc/Rpb3 ratio at the *ARG1* gene. (E) Spt6-Myc occupancy at the core promoter (TATA), 5′ (5′ORF), and 3′ (3′ORF) parts of the *ADH1* gene. The signal for *ARG1* and *ADH1* ChIP DNA was normalized to their respective input DNA (ChIP/Input) and further normalized against the *POL1* ChIP/input ratios. ChIPs were conducted using at least three independent cultures, and the error bars represent the standard errors of the mean (SEM). (F and G) Western blots showing the levels of Myc-tagged Spt6 (F) and untagged Spt6 (G) in WT and Ser2 kinase mutant strains. Proteins from the indicated strains were extracted using the TCA method after a 1-h treatment with 3MB-PP1. Gcd6 was used as a loading control. The band intensities were quantified by using Image Studio Lite (LI-COR Biosciences), and the average data from three independent cultures and two different loadings from each sample were plotted and are shown below the blots. Error bars indicate the SEM.

specific) CTD repeats by Bur1 and Ctk1 near the 5′ORF, rather than bulk levels of Ser2 phosphorylation, is important for the efficient recruitment of Spt6.

To further determine whether highly transcribed genes are more reliant on Ser2 kinases for recruiting Spt6, we analyzed these genes based on Rpb3 occupancy (see Table S1 in the supplemental material). Unlike the Rpb3 defect that uniformly extends along the entire ORF (Fig. 2D, left panel), reduction in Spt6 occupancy was more pronounced near the 5′ end (Fig. 2D, right panel) of the genes, irrespective of Rpb3 occupancy. The role of Ser2P in recruiting Spt6 was even more evident for genes containing <0.5 $\log_2$ Rpb3 occupancy (Fig. 2E; see Table S1 in the supplemental material), indicating that Ser2 kinases are essential for recruiting Spt6 at the 5′ORFs of genes transcribed at low levels (low-transcribed genes) as well.

It was surprising to see that Spt6 binding around the transcription end site (TES) was largely unaffected in the Ser2 double kinase mutant (Fig. 2C to E), despite the loss from the 5′ORF. This observation suggests that Spt6 recruitment toward the 3′ end of the gene is carried out by other mechanisms, whereas Ser2 kinases are required for promoting Spt6 recruitment to the 5′ ends of genes. Tyr1-CTD phosphorylation, which has the greatest affinity to the Spt6 tSH2 domain *in vitro* (23) and peaks at the 3′ ends of genes, may facilitate Spt6 recruitment toward the end of the ORF in the absence of Ser2P, since Tyr1P levels are not affected by the known Pol II CTD kinases (23).

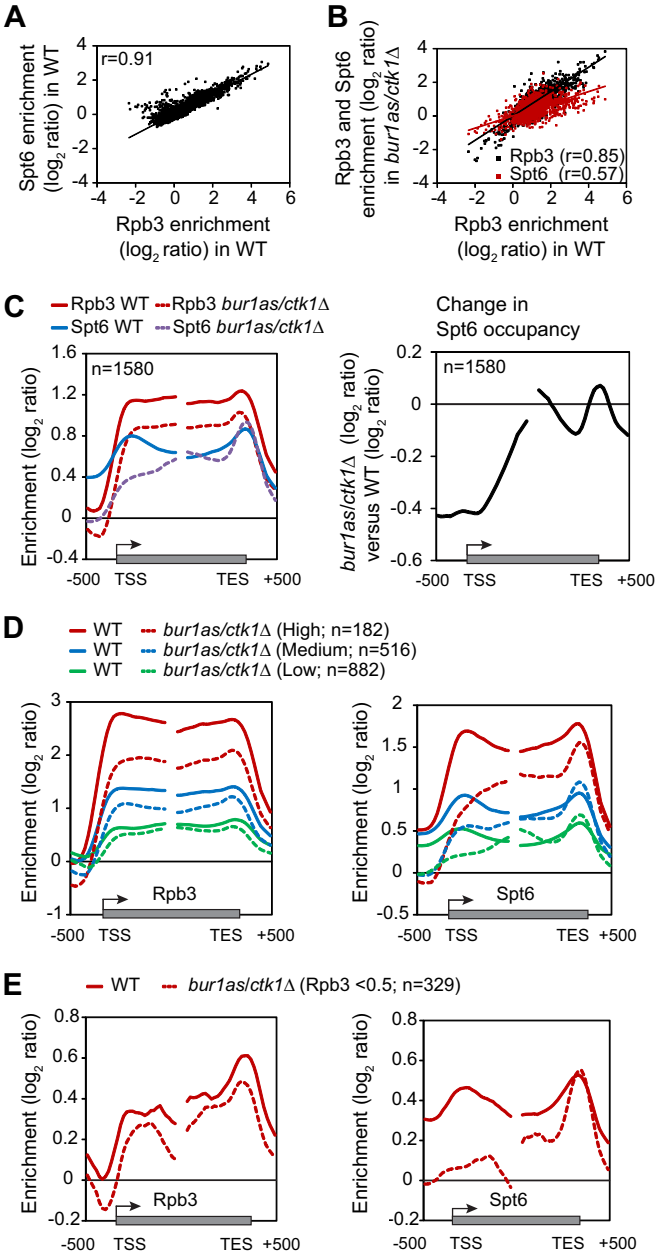

FIG 2 Ser2 kinases promote Spt6 recruitment to the 5′ORFs. (A) Log_2 enrichment ratios for Spt6 and Rpb3 in WT cells were averaged over the transcribed regions, and Spt6 values were plotted against Rpb3 values for each gene (>6,000 genes). (B) Scatter plot of the average log_2 enrichment ratio of Rpb3 and Spt6 in the *bur1as/ctk1*Δ mutant against the average Rpb3 log_2 enrichment ratio in WT cells for the top 25% Spt6-occupied genes (n = 1,580). The Pearson correlation coefficients (r) are indicated. (C) The log_2 enrichment ratio of Rpb3 and Spt6 across metagenes made of the top 25% Spt6-occupied genes in WT and *bur1as/ctk1*Δ cells is shown on the left. The change in the Spt6 log_2 enrichment ratio (mutant − WT) is shown on the right. The box at the bottom of the plots represents the transcribed region. The transcription start site (TSS) and transcription end site (TES) are marked. (D) Rpb3 (left) and Spt6 (right) log_2 enrichment ratio in WT and *bur1as/ctk1*Δ cells along groups of Spt6-occupied genes with different Rpb3 average log_2 enrichment ratios (>2, high; between 1 and 2, medium; <1, low). (E) Rpb3 (left) and Spt6 (right) log_2 enrichment ratio in WT and *bur1as/ctk1*Δ cells along genes with Rpb3 average log_2 enrichment ratios of <0.5. The number of genes in each group is indicated.

Spt6 occupancy is not impaired in Ser5 kinase mutants. Given that the Spt6 tSH2 domain strongly binds to Ser5-phosphorylated (Ser5P) but not to unmodified CTD peptides and that a stronger binding is observed with doubly phosphorylated CTD peptides (Ser2P/Ser5P or Tyr1P/Ser5P) (23–25), we examined whether Ser5 phosphorylation alone, or in combination with Ser2P, plays a role in recruiting Spt6. To this end, we measured Spt6 binding in *kin28as* and *kin28as/bur2*Δ mutants. As expected, treating these mutants with the ATP analog NA-PP1 substantially reduced Ser5P across the *ARG1*, *ADH1*, and *PMA1* genes (Fig. 3A and data not shown). In contrast, Spt6 and Rpb3 occupancies at *ARG1* were similar to that of WT in these mutants (Fig. 3B and C), indicating that Ser5P by Kin28 is dispensable for Spt6 recruitment. A small reduction in Spt6 binding at *ADH1* and a substantial reduction in the *PMA1* gene (Fig. 3D and F) could be attributed to the reduced Pol II in these mutants (Fig. 3E and G). As such, the Spt6-Myc/Rpb3 ratios in the kinase mutants were largely similar to the WT, except for a slight reduction in the ratio at the 3′ORF of *PMA1* (Fig. 3H). Collectively, these data suggest that Ser5 phosphorylation by Kin28 is not significantly required for recruiting Spt6 to these genes.

To evaluate the role of Ser5 phosphorylation genome-wide, we examined Spt6-Myc occupancy in the *kin28as/bur2*Δ mutant by using ChIP-chip experiments. We selected this mutant because deleting *BUR2* in the *kin28as* background elicits greater reductions in Ser5 phosphorylation than *kin28as* alone (29). To determine whether Spt6 occupancy is affected in *kin28as/bur2*Δ cells, we calculated the average Spt6 occupancy over each transcribed region, selected the top 25% of the Spt6-occupied genes (n = 1,580) (see Table S2 in the supplemental material), and plotted the average Rpb3 and Spt6 log_2 values for these genes. Rpb3 occupancy in the mutant closely followed that of WT until the TSS and then showed a sharp decline in the ORF of the metagene (Fig. 3I). As previously observed (29, 44–46), the sharp reduction in Rpb3 occupancy downstream of the TSS in various Kin28 mutants is more consistent with a promoter clearance defect than with a Pol II processivity defect, as the latter would have produced a gradual reduction in Rpb3 binding. Similarly, Spt6 occupancy was reduced in the ORF (Fig. 3I), which can be attributed to the Pol II binding defect. Overall, these data are consistent with the gene-specific ChIP results (Fig. 3B, D, and F) and suggest that the *kin28as/bur2*Δ mutant has a minor, if any, effect on Spt6 occupancy. Further analyses of Spt6 binding at genes binned based on their Rpb3 occupancy (high, medium, and low) (see Table S2 in the supplemental material) showed that Spt6 binding defect mirrors the reduction in Pol II (Fig. 3J). Altogether, our data show that Ser5 phosphorylation indirectly regulates Spt6 binding by modulating Pol II occupancy *in vivo*.

Spt6 is required for maintaining histone occupancy in coding regions. To investigate whether Spt6 regulates histone density in the coding regions, we measured histone occupancy at the *ARG1* ORF in Spt6-depleted cells. We utilized a strain in which *SPT6* expression is driven by a tetracycline-titratable promoter (*SPT6-tet*) (33) and is repressed in the presence of doxycycline (Dox). Dox-treated *SPT6-tet* cells revealed a substantial reduction in total Spt6 levels (Fig. 4A). Depletion of Spt6 (Dox-treated) led to a greater reduction in H3 occupancy in the *ARG1* 3′ORF under inducing conditions (Fig. 4B, compare induced No Dox and Dox), a finding consistent with the role of Spt6 in regulating histone occupancy. This reduction, in part, stems from the failure of

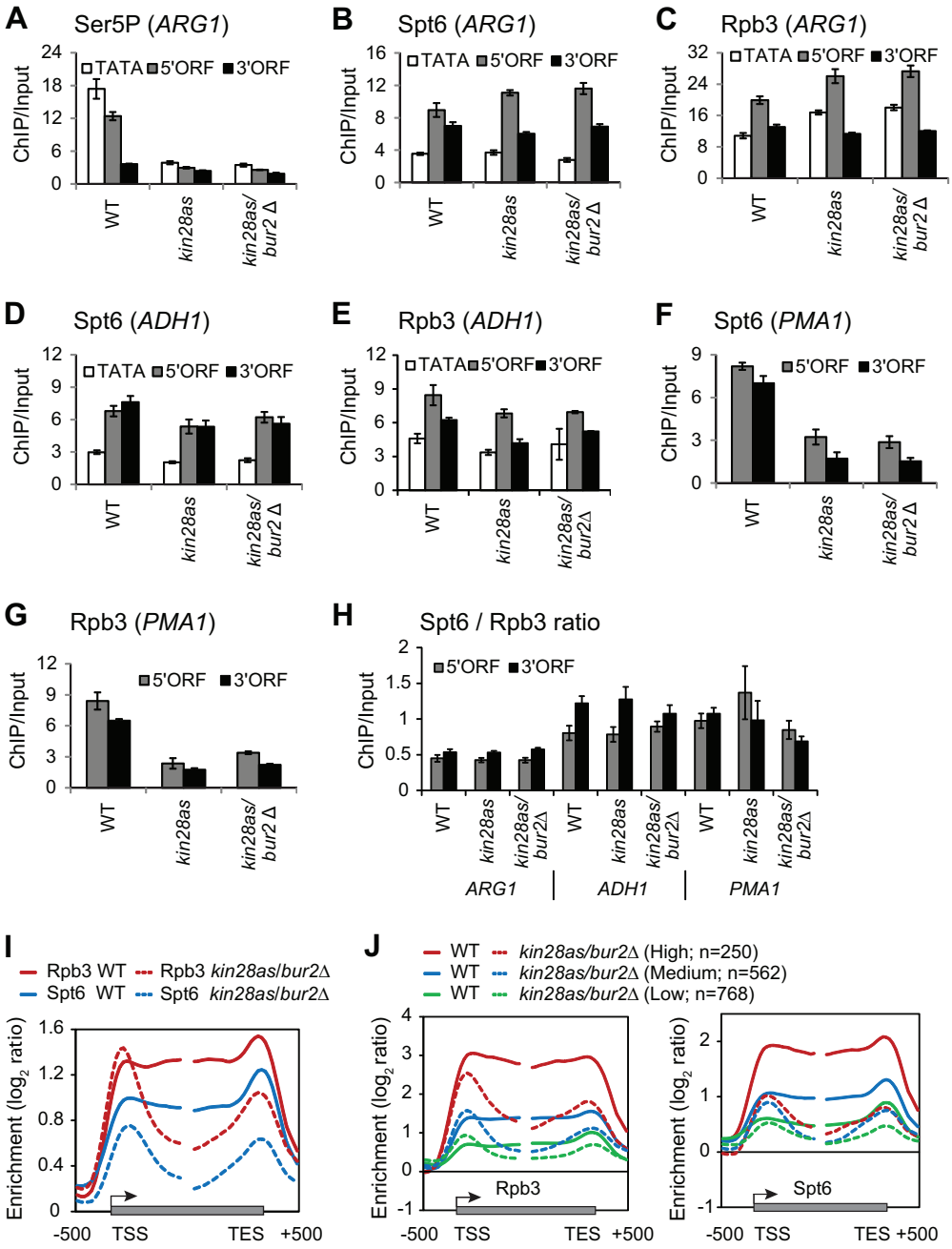

FIG 3 Ser5 kinases are dispensable for Spt6 recruitment. Cells were treated with 6 μM NA-PP1 to inactivate Kin28 and processed for ChIP. The occupancy of Ser5P, Spt6-Myc, and Rpb3 (Pol II) was determined for WT, *kin28as*, and *kin28as*/*bur2*Δ cells. The occupancy of Ser5P (A), of Spt6-Myc (B), and of Rpb3 (C) is shown for the *ARG1* gene. (D and E) ChIP occupancy of Spt6-Myc (D) and of Rpb3 (E) across the *ADH1* gene. (F and G) ChIP occupancy of Spt6-Myc (F) and of Rpb3 (G) at the 5′ and 3′ ends of *PMA1*. (H) The Spt6-Myc occupancies at the 5′ and 3′ ORFs were normalized to the Rpb3 occupancies at these regions, and the Spt6-Myc/Rpb3 ratios are shown for *ARG1*, *ADH1*, and *PMA1*. (I) Metagene analysis showing Rpb3 and Spt6 $\log_2$ enrichment ratios in WT and *kin28as*/*bur2*Δ for the top 25% of the Spt6-occupied genes ($n = 1{,}580$; selected based on the average Spt6 binding in the coding region of each gene). The box at the bottom of the plots represents the transcribed region. The TSS and TES are marked. (J) Log_2 enrichment ratios for Rpb3 (left) and Spt6 (right) on genes binned based on their average Rpb3 occupancy in the coding region are indicated (>2, high; between 1 and 2, medium; <1, low). The number of the genes in each group is also indicated.

histones to fully recover upon repression to the levels observed prior to *ARG1* induction (Fig. 4B, compare repressed No Dox and Dox) in Spt6-depleted cells. This is unlikely due to sustained transcription of *ARG1* in Spt6-depleted cells because Rpb3 binding was reduced to a noninducing level upon repression (Fig. 4C). Overall, our data indicate that Spt6 is dispensable for regulating Pol II occupancy at the *ARG1* gene. It is, however, needed to maintain normal cotranscriptional histone occupancy in the coding region. Interestingly, the reduction in H3 occupancy in the *ARG1* ORF resembled that of strains lacking histone deacetylases (35,

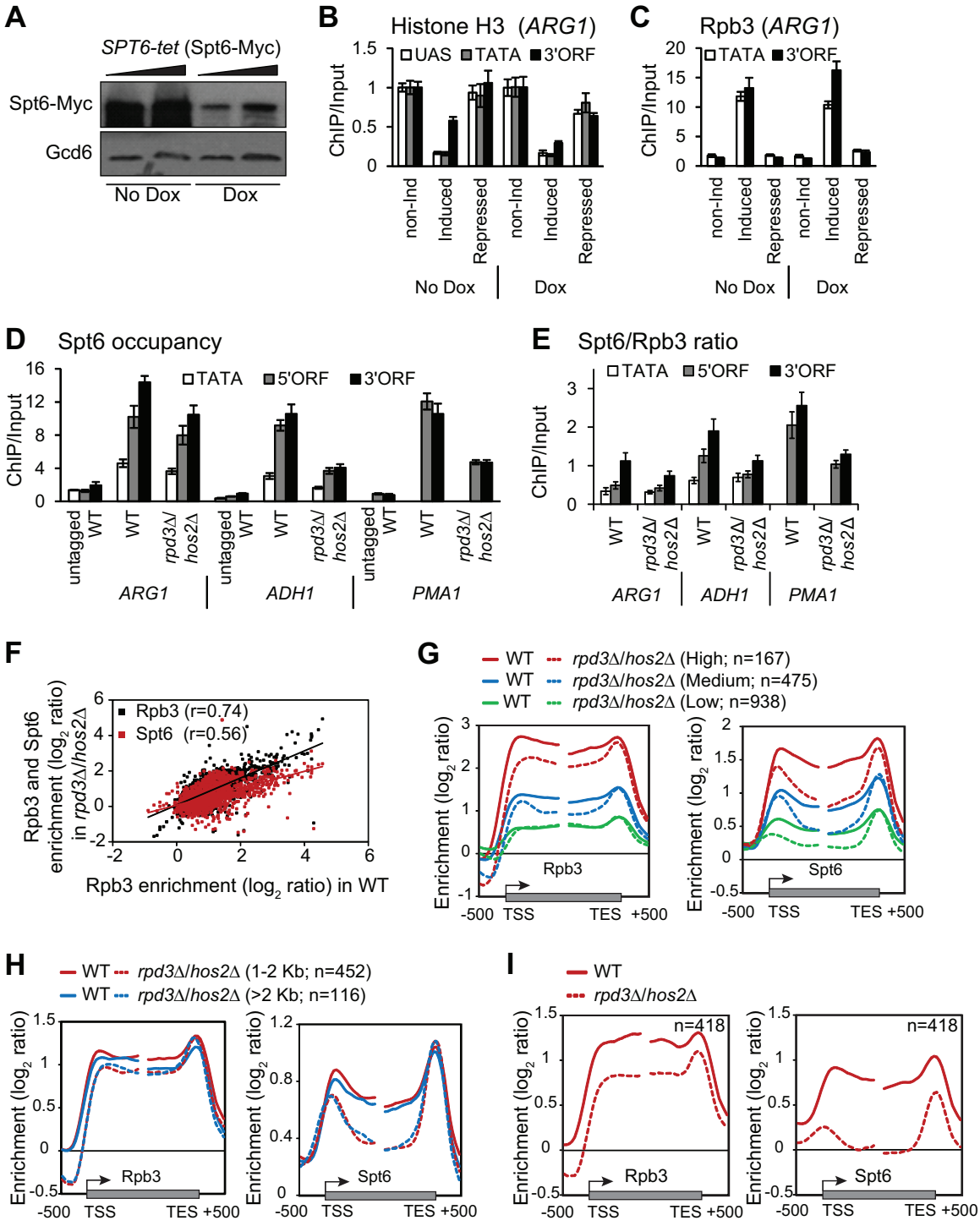

FIG 4 HDACs promote Spt6 recruitment to the coding regions. (A) *SPT6-tet* cells carrying a Myc-tagged Spt6 were grown in SC plus 10 μg of doxycycline (Dox)/ml overnight and subcultured in the presence of 10 μg of Dox/ml the next day. Cells were treated with SM to induce Gcn4 targeted genes and processed for ChIP as described in the legend of Fig. 1. A fraction of the cells (10 ml) was collected prior to the cross-linking step, and TCA-precipitated whole-cell extracts were used to determine Spt6-Myc levels by Western blotting with anti-Myc antibodies. "Dox" and "No Dox" represent cells treated and not treated with doxycycline, respectively. Gdc6 was used as a loading control. (B and C) Histone H3 (B) and Rpb3(C) occupancy at the upstream activating sequence (UAS), the promoter (TATA), and the coding region (3′ORF) of the *ARG1* gene with (Dox) or without (No Dox) doxycycline treatment under noninduced, induced, and repressed conditions. A 10× isoleucine-valine solution was added to the induced cells for 5 min to repress *ARG1* transcription. (D) Spt6 occupancy in WT and *rpd3*Δ/*hos2*Δ cells at the *ARG1*, *ADH1*, and *PMA1* genes. (E) Spt6-Myc/Rpb3 ratio along the *ARG1*, *ADH1*, and *PMA1* genes. (F) Scatter plot of Rpb3 and Spt6 $\log_2$ enrichment ratio in *rpd3*Δ/*hos2*Δ cells against the Rpb3 $\log_2$ enrichment in WT cells for the top25% Spt6-occupied genes. The Pearson correlation coefficient (*r*) is indicated in parentheses. (G) Rpb3 (left) and Spt6 (right) $\log_2$ enrichment ratio in WT and *rpd3*Δ/*hos2*Δ cells on groups of genes binned based on their Rpb3 average $\log_2$ enrichment levels. The box at the bottom of the plots represents the transcribed region. The TSS and TES are marked. (H) Rpb3 (left) and Spt6 (right) average $\log_2$ enrichment ratio in WT and *rpd3*Δ/*hos2*Δ cells along genes with gene lengths of >2 kb or between 1 and 2 kb. (I) Rpb3 (left) and Spt6 (right) $\log_2$ enrichment ratio in WT and *rpd3*Δ/*hos2*Δ cells at 418 genes showing a >0.5 reduction in the Spt6 $\log_2$ binding ratio.

47), suggesting that HDACs function with Spt6 to maintain appropriate nucleosome occupancy. This is consistent with the fact that mutations in Spt6, Rpd3S, and Hos2-Set3 complexes result in spurious transcription from many genes (17, 18, 21, 48).

HDACs promote Spt6 recruitment. To test whether HDACs promote Spt6 occupancy in the ORFs of transcribed genes, we examined the recruitment of Spt6-Myc in the HDAC *rpd3*Δ/*hos2*Δ mutant. This mutant revealed a small (~25%) reduction in Spt6-Myc binding at the *ARG1* 3′ORF (Fig. 4D). Interestingly, the *rpd3*Δ/*hos2*Δ mutation elicited greater reductions (2- to 2.5-fold) in Spt6 binding to the coding regions of constitutively expressed *ADH1* and *PMA1* genes (Fig. 4D). Since we observed a small Rpb3 binding defect at these genes, we calculated the Spt6-Myc/Rpb3 ratios and found that they were reduced in the coding regions of the *ARG1*, *ADH1*, and *PMA1* genes (Fig. 4E). The *rpd3*Δ/*hos2*Δ double mutant produced greater defects in Spt6 binding and H3 occupancy (35) than the single mutants (data not shown). Collectively, these data suggest that both Rpd3 and Hos2 are needed for full recruitment of Spt6 to the coding regions.

To further define the role of these HDACs in Spt6 recruitment, we determined the genome-wide occupancy of Spt6 and Rpb3 in WT and *rpd3*Δ/*hos2*Δ cells by ChIP-chip analysis (see Table S3 in the supplemental material). While Rpb3 showed a strong correlation between WT and the double mutant for the top 25% Spt6-occupied genes, Spt6 in the mutant only modestly correlated with Rpb3 in WT cells (Fig. 4F). This suggests a role for these HDACs in Spt6 recruitment. Spt6-bound genes were grouped into high-, medium-, and low-transcribed genes based on the average Rpb3 occupancy in the ORF. Although the *rpd3*Δ/*hos2*Δ mutant produced a small reduction in Rpb3 binding across the metagene of the high and medium groups, the low-transcribed group was largely unaffected (Fig. 4G, left panel). In contrast to the uniform reduction in Rpb3 across the ORF, the reduction in Spt6 binding in the *rpd3*Δ/*hos2*Δ mutant was mostly localized to the middle of the transcribed region (Fig. 4G, right panel). This was even more apparent in the low-transcribed group, which has the WT levels of Rpb3. This suggests that HDACs potentially regulate Spt6 occupancy in the midtranscribed ORFs after initial recruitment to the 5′ end. To determine whether the role of HDACs in regulating Spt6 occupancy depends on gene length, we plotted Spt6 occupancy at genes with medium (1 to 2 kb, $n = 452$) and long (>2 kb, $n = 116$) ORFs (see Table S3 in the supplemental material). Compared to a slight reduction in Rpb3, Spt6 occupancy in the *rpd3*Δ/*hos2*Δ mutant was greatly diminished from the middle of coding regions for both groups of genes (Fig. 4H). This observation provides further support to the idea that HDACs maintain Spt6 association in the coding region after initial recruitment. Furthermore, we identified 418 genes in which Spt6 was reduced (≥0.5 $\log_2$) in the HDAC mutant (see Table S3 in the supplemental material) and plotted the Rpb3 and Spt6 occupancies. Although these genes showed an overall Rpb3 binding defect, the Spt6 binding was diminished to nearly background levels in the coding region (Fig. 4I). Interestingly, even at these genes, a distinct Spt6 binding peak can be observed near the TES, suggesting that Spt6 is recruited near the transcription end sites in a manner independent of HDACs or Ser2 kinases. In summary, our data indicate that HDACs Rpd3 and Hos2 regulate Spt6 occupancy in coding regions. Unlike Ser2 kinases, Rpd3 and Hos2 appear to function in sustaining high levels of Spt6 occupancy in the mid-transcribed regions following the recruitment to the 5′ proximal region.

HDACs promote Spt6 interaction with phosphorylated Pol II CTD. Since Spt6 interacts with phosphorylated Pol II, an impaired Spt6-Pol II interaction could account for the reduced Spt6 association in the mid-transcribed regions. To test this, we immunoprecipitated Spt6-Myc and examined for the presence of phosphorylated Ser2 and Ser5 in the immunoprecipitates. Consistent with the proposed interaction of Spt6 with elongating Pol II, Ser2P and Ser5P coimmunoprecipitated with Spt6-Myc from the WT but not with the Myc-tagged Rli1 (Rli1-Myc), a translation factor used as a control (Fig. 5A). Interestingly, phosphorylated forms of Pol II were greatly diminished in Spt6-Myc immunoprecipitates from the *rpd3*Δ/*hos2*Δ mutant despite having WT levels of Ser2P and Ser5P (Fig. 5A, Ser2P and Ser5P inputs). These results suggest that Rpd3 and/or Hos2 promote association of Spt6 with the phospho-Pol II CTD.

The simplest explanation for both the diminished coimmunoprecipitation of phosphorylated Pol II with Spt6 (Fig. 5A) and the reduced Spt6 binding in the coding regions in the *rpd3*Δ/*hos2*Δ mutant (Fig. 4G to I) is that these HDACs facilitate Spt6 association with the transcribed regions by stabilizing its interaction with phosphorylated Pol II. Given that both Rpd3S and Hos2-Set3 complexes deacetylate ORF nucleosomes (47–49), it is possible that hyperacetylation of the ORF nucleosomes in *rpd3*Δ/*hos2*Δ suppresses Spt6 binding. To test this, we examined Spt6 occupancy in *set1*Δ, *set2*Δ and *set1*Δ/*set2*Δ mutants. Set1 and Set2 methylate H3K4 and H3K36, respectively, and these methylated residues are required for Hos2-Set3C and Rpd3S binding and subsequently for deacetylation of the ORF nucleosomes (35, 47, 48). Unlike reduced Spt6 binding seen in *rpd3*Δ/*hos2*Δ (Fig. 4D), the binding in the *ADH1* and *PMA1* coding regions was not affected in *set1*Δ cells and was only slightly reduced in the *set2*Δ and *set1*Δ/*set2*Δ mutants (Fig. 5B). A small reduction in binding was also seen at the *ARG1* ORF in the *set1*Δ/*set2*Δ mutant (Fig. 5D). Rpb3 occupancy in the single mutants was similar to that observed in the WT (Fig. 5C and E) and was slightly reduced in the *set1*Δ/*set2*Δ double mutant. Overall, histone methyltransferase mutants exhibited only a small reduction in Spt6 binding. To confirm that acetylation is in fact increased in these histone methyltransferase mutants under our experimental conditions, we analyzed both H3 and H4 acetylation in these mutants. We found that both H3 aand H4 acetylation increased in the 3′ORFs of *STE11* and *FLO8* in the mutants (Fig. 5F and G). The increase in H3 and H4 acetylation in the *set1*Δ/*set2*Δ mutant was largely similar to that observed in the *set2*Δ single mutant, except for the acetylated H3 at the *STE11* 3′ORF, where it appears that both Set1 and Set2 cooperate to regulate histone acetylation. Likewise, the histone acetylation was also increased by ~1.5- to 2-fold in the coding regions of *PMA1* in the *set1*Δ/*set2*Δ mutant (Fig. 5H). An increase in H3 acetylation, though to a lesser degree, was also observed at the *ADH1* ORF in these mutants (data not shown). Our results showing increased histone acetylation in the methyltransferase mutants are consistent with previous studies (20, 47, 48) and indicate that impaired Spt6 binding in the *rpd3*Δ/*hos2*Δ mutant cannot be accounted for simply by altered histone acetylation in this mutant. Furthermore, a greater reduction in Spt6 occupancy in *rpd3*Δ/*hos2*Δ cells than that observed in *set1*Δ/*set2*Δ cells suggests that HDACs regulate Spt6 association with Pol II before deacetylation of nucleosomes. To test this, we immunoprecipitated Spt6-Myc from the WT and *set1*Δ/*set2*Δ cells and probed for Ser5P and total Pol II (Rpb3). Both Rpb3 and Ser5P were efficiently coimmunoprecipitated

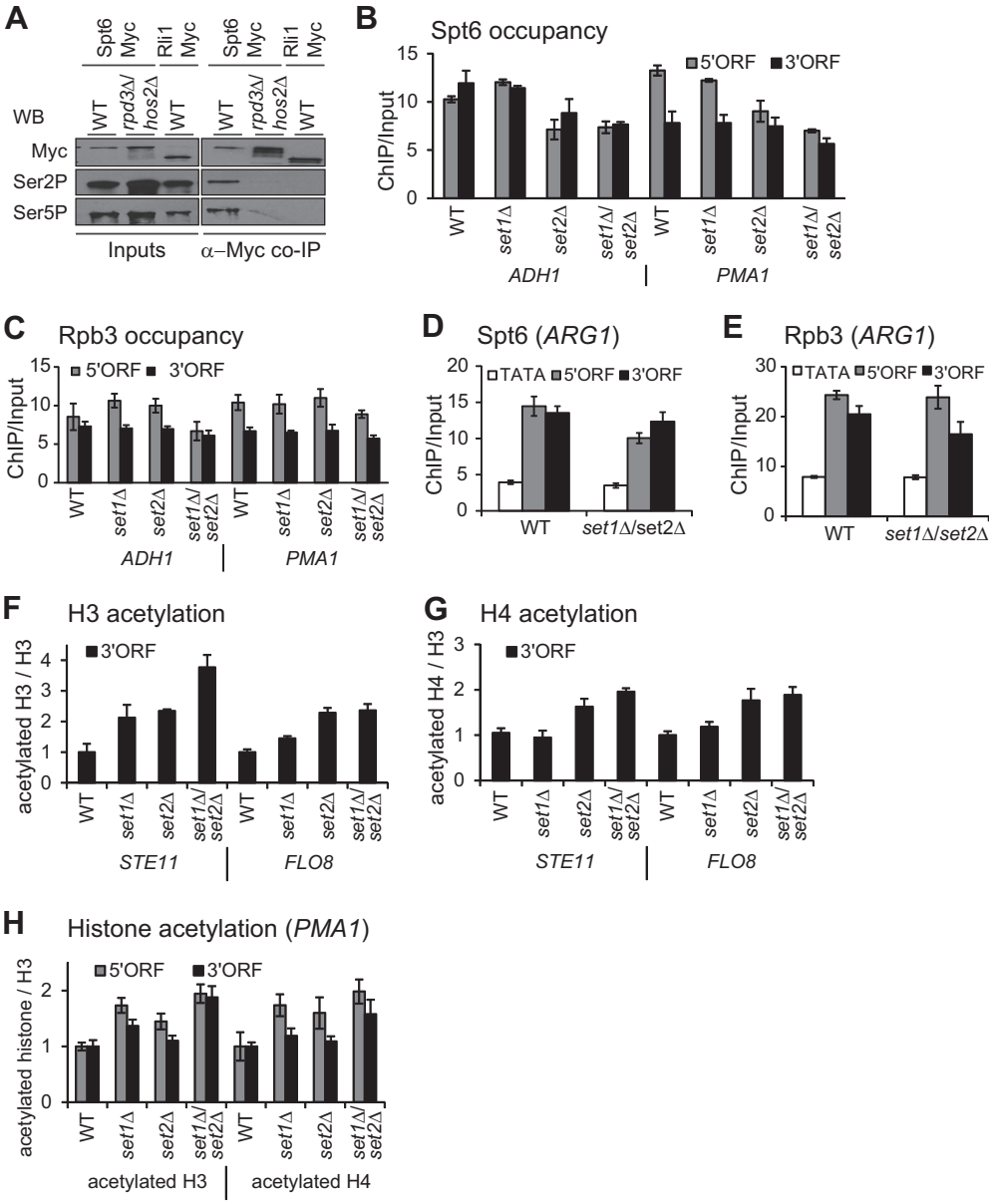

FIG 5 Histone methyltransferases are not required for Spt6 recruitment. (A) Whole-cell extracts prepared from Spt6-Myc tagged WT and *rpd3*Δ/*hos2*Δ strains were immunoprecipitated with anti-Myc antibodies, and the immunoprecipitates were then subjected to Western blot analysis with antibodies against Myc, Ser2P, and Ser5P. Rli1-Myc was used as a control. (B and C) Spt6-Myc (B) and Rpb3 (C) occupancy in the 5′ (5′ORF) and 3′ (3′ORF) part of the *ADH1* and *PMA1* coding regions in the indicated histone methyltransferase mutants. (D and E) Spt6-Myc (D) and Rpb3 (E) enrichment at the *ARG1* gene in WT and *set1*Δ/*set2*Δ cells. (F to H) The ChIP occupancies of acetylated H3 and H4 were normalized to the H3 occupancies. The levels of H3 acetylation/H3 (F) and H4 acetylation/H3 (G) at the 3′ORF of the *STE11* and *FLO8* genes and at the 5′ORF and 3′ORF of *PMA1* (H) are shown.

from the WT and *set1*Δ/*set2*Δ extracts (Fig. 6A), indicating that Set1 and Set2 (or methylation-dependent deacetylation) are dispensable for Spt6-Pol II interaction.

To further examine whether hyperacetylation inhibits Spt6 binding, we performed histone N-terminal tail peptide pulldown assays. Both unmodified and acetylated (ac) H3 and H4 peptides precipitated similar amounts of Spt6-Myc from whole-cell extracts prepared from the Spt6-Myc tagged strain (Fig. 6B). Myc signals were not detected in the pulldown experiments using Rli1-Myc or untagged WT strains (Fig. 6B). These results show that Spt6 interaction with H3 and H4 N-terminal tails do not strongly depend on acetylation. In further support of this observation, deleting 1 to 16 residues of H4 (Δ1-16 H4) or a larger deletion (Δ1-24 H4), which removes all the acetylable residues within the H4 tail (K5, K8, K12, and K16), did not significantly reduce Spt6 occupancy in the *PMA1* or *ADH1* ORFs (Fig. 6C). Similarly, deleting H3 N-terminal tail, which eliminates acetylable lysines within the H3 tail (H3 K9, K14, K18, K23, and K27) also failed to reduce Spt6 occupancy in the ORFs of *ADH1* and *PMA1* (Fig. 6D, left). Consistent with this, the H3K→A mutant (H3 K4, K9, K14, and K18 substituted to alanines) displayed WT levels of Spt6-Myc occupancy at the *PMA1* ORF and elicited only a minor reduction

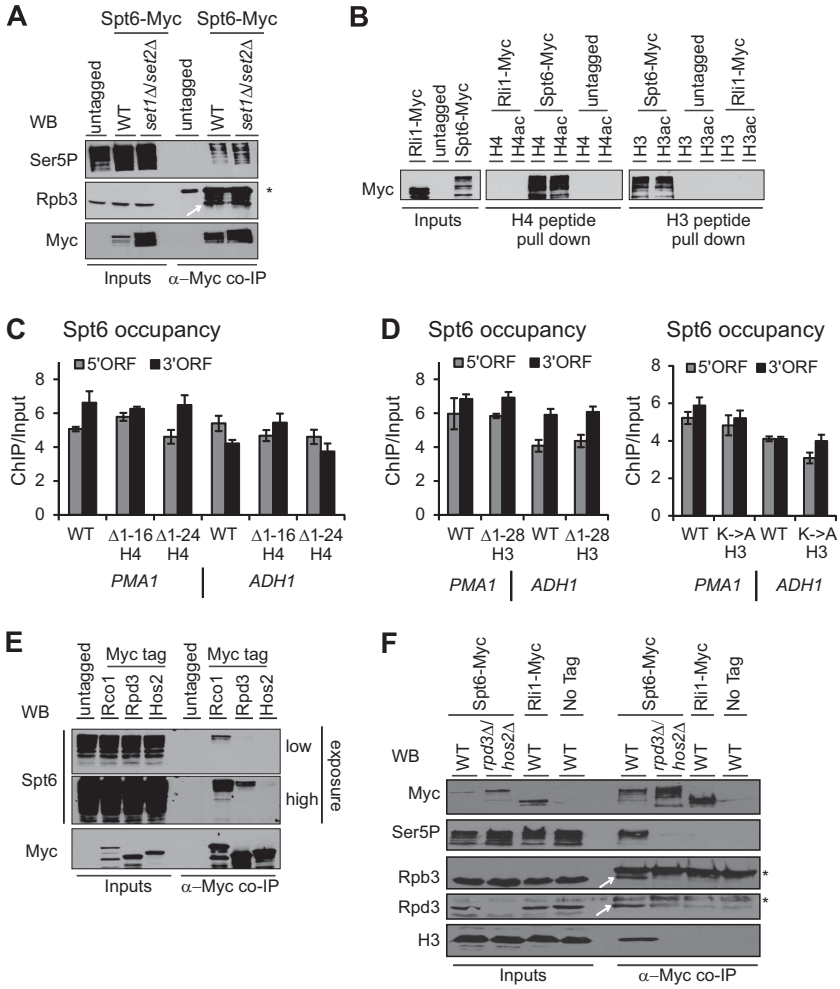

FIG 6 HDACs promote Spt6-Pol II interaction independently of histone acetylation. (A) Spt6-Myc was immunoprecipitated from whole-cell extracts prepared from WT and *set1*Δ/*set2*Δ cells, and Ser5P and Rpb3 were detected in the immunoprecipitates by Western blotting. (B) H3, acetylated H3 (H3ac), H4, and acetylated H4 (H4ac) histone N-terminal tail peptides were used in peptide pulldown experiment using whole-cell extracts prepared from Spt6-Myc- or Rli1-Myc (used as a control)-tagged strains. An untagged strain was additionally used as a negative control. (C) Spt6-Myc ChIP occupancy at the 5′ORF and 3′ORF of *ADH1* and *PMA1* in the histone H4 tail deletion mutants. (D) Spt6-Myc ChIP occupancy at the 5′ORF and 3′ORF of the *PMA1* and *ADH1* genes in the H3 tail deletion mutant (H3 Δ1-28) (left panel) and H3 K⟶A mutant (right panel). (E) Whole-cell extracts prepared from Myc-tagged Rco1, Rpd3, and Hos2 and an untagged strain were immunoprecipitated with anti-Myc antibodies, and Spt6 was detected using anti-spt6 antibodies. (F) Spt6-Myc was immunoprecipitated with anti-Myc antibodies from whole-cell extracts of WT and *rpd3*Δ/*hos2*Δ cells, and Ser5P, Rpb3, Rpd3, and H3 were detected by Western blotting. Rli1-Myc and untagged WT strain were used as a negative control. The specific Rpb3 and Rpd3 bands are indicated by arrows, and the IgG bands are indicated by asterisks in panels A and F.

in Spt6-Myc binding at the *ADH1* 5′ORF (Fig. 6D, right). These last results are in agreement with a previous study (50) showing that histone H3 tail is not required for Spt6 recruitment at the *RNR3* gene. These results imply that both H3 and H4 N-terminal tails are dispensable for recruiting Spt6 to the transcribed regions of these genes and that HDACs maintain Spt6 association to the transcribed region by promoting Spt6-Pol II interactions.

Considering that phosphorylated Pol II recruits HDACs Rpd3S and Hos2 (35, 51), as well as Spt6, to the transcribed regions (Fig. 1 to 4), we hypothesized that Spt6-HDAC interactions promote the association of Spt6 with transcribed genes. To this end, we immunoprecipitated Myc-tagged Rpd3, Rco1 (a subunit specific to Rpd3S), and Hos2 and examined the coimmunoprecipitation of Spt6 by Western blot analysis. Spt6 coimmunoprecipitated with Rco1 and, to a lesser extent, with Rpd3 but not with Hos2 or the untagged WT used as a control (Fig. 6E). This suggests that Rpd3-containing complexes are largely responsible for promoting Spt6-Pol II interactions. However, the single *rpd3*Δ mutant failed to impair Spt6-Pol II interaction (data not shown), suggesting that both Rpd3 and Hos2 are promoting this interaction. These results are in agreement with the observation that the *rpd3*Δ/*hos2*Δ mutant produced a greater reduction in Spt6 occupancy at *ADH1* and *PMA1* ORFs than the respective single mutants (data not shown).

We considered the possibility that the lack of Spt6 interaction with the elongating Pol II also diminishes its interaction with histones. To test this, we immunoprecipitated Spt6-Myc and examined the coimmunoprecipitation of histone H3. Consistent with our earlier observations (Fig. 5A and 6A, and E), coimmunoprecipitation of Ser5P, Rpb3, and Rpd3 was seen with Spt6-Myc in

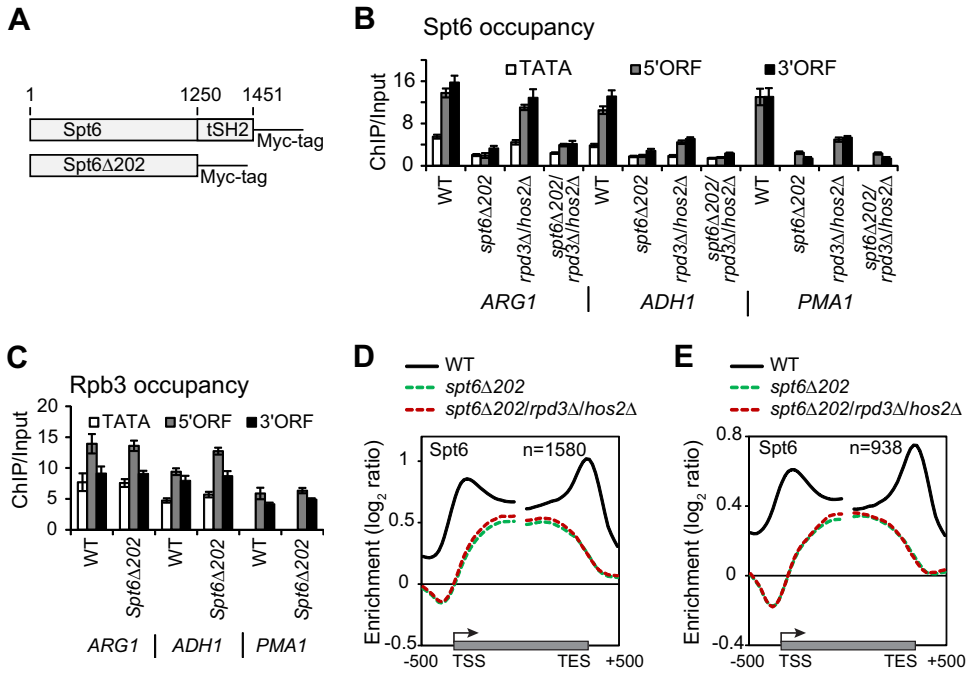

FIG 7 CTD kinases and HDACs coordinate Spt6 recruitment. (A) Schematic diagram of Spt6 with tSH2 showing the amino acids deleted to obtain the *spt6Δ202* mutant. (B) ChIP occupancy of Spt6-Myc in WT, *spt6Δ202*, *rpd3Δ/hos2Δ*, and *spt6Δ202/rpd3Δ/hos2Δ* cells at the *ARG1*, *ADH1*, and *PMA1* genes. (C) Rpb3 occupancy in WT and *spt6Δ202* cells at the *ARG1*, *ADH1*, and *PMA1* genes. (D) Average $\log_2$ enrichment of Spt6 at the top 25% Spt6-occupied genes in WT, *spt6Δ202*, and *spt6Δ202/rpd3Δ/hos2Δ* cells. The box at the bottom of the plots represents the transcribed region. The TSS and TES are marked. (E) Average $\log_2$ enrichment of Spt6 at low-transcribed genes affected in the *rpd3Δ/hos2Δ* mutant in WT, *spt6Δ202*, and *spt6Δ202/rpd3Δ/hos2Δ* cells.

the WT cells but not in *rpd3Δ/hos2Δ* cells (Fig. 6F). Similarly, H3 was observed in immunoprecipitates from the WT but not from the HDAC mutant, indicating that the Spt6 interaction with Pol II is needed for efficient interaction with histones. Altogether, our results support a model in which initial recruitment of Spt6 by Ser2 CTD kinases near the TSS is maintained by HDACs across the transcribed region and that interactions between HDACs and Spt6 contribute to this process.

HDACs and CTD kinases coordinate Spt6 recruitment. Considering that *rpd3Δ/hos2Δ* impairs Spt6-Pol II interactions (Fig. 5A and 6F) and reduces Spt6 occupancy downstream of TSS genome-wide (Fig. 4G to I), it is possible that HDACs are needed to maintain Spt6 binding after CTD-dependent recruitment at the 5′ORF. Alternatively, HDACs could independently recruit Spt6 to the mid-transcribed regions. To distinguish between these two possibilities, we deleted the tSH2 domain (*spt6Δ202*) in WT and *rpd3Δ/hos2Δ* cells and examined the occupancy of this Spt6 mutant (Fig. 7A). Since the tSH2 domain interacts with the phosphorylated CTD (24–26), deleting this domain should diminish CTD-dependent Spt6 recruitment. In agreement with a previous study (22), deleting the tSH2 greatly reduced Spt6 but not Pol II (Rpb3) occupancy in the *ARG1*, *ADH1*, and *PMA1* coding regions (Fig. 7B and C). However, the *rpd3Δ/hos2Δ* mutation did not cause any further reduction in Spt6Δ202-Myc occupancy at these genes, supporting the idea that HDACs stabilize Spt6 association rather than independently recruit Spt6 in coding regions. This is further supported by ChIP-chip experiments showing that the Spt6Δ202-Myc binding profile in WT cells was almost identical to that of *rpd3Δ/hos2Δ* cells at the top 25% Spt6 occupied genes, as well as at low-expressed genes (Fig. 7D and E; see Table S4 in the supplemental material). Comparing the Spt6-Myc binding profile to that of Spt6Δ202-Myc revealed a significantly reduced Spt6 binding peak around the TSS. The Spt6-Myc binding around the TES, which was largely unaffected in *bur1as/ctk1Δ* and in *rpd3Δ/hos2Δ* mutants, was strikingly reduced in the *spt6Δ202* mutant, indicating that the tSH2 domain is essential for recruiting Spt6 near the TSS, as well as near the TES. The fact that tSH2 recognizes both Ser2/Ser5 and Tyr1 phosphorylated CTD (23–25), combined with the fact that tSH2 deletion, but not inactivation, of Ser2 kinases (Fig. 2C to E) reduced Spt6 binding near the TES, strongly suggests that phosphorylated Tyr1 is needed for recruiting Spt6 in this region. Because the kinase responsible for phosphorylating Tyr1 is not yet identified in *S. cerevisiae*, we were unable to directly determine whether this phosphorylation is needed for Spt6 recruitment *in vivo*.

DISCUSSION

In this study, we investigated the mechanisms by which Spt6 is recruited to the coding regions of transcribed genes. We report that both Ser2 CTD kinases and HDACs coordinate Spt6 association to different regions of the transcribed genes. Our results revealed that the Pol II CTD phosphorylated at Ser2 is important for recruiting Spt6 to the 5′ORF. This CTD-dependent recruitment is, surprisingly, insufficient to maintain the high levels of Spt6 binding that is seen on transcribed regions. We provide evidence for an unexpected role of HDACs in sustaining high occupancy of Spt6 in transcribed ORFs by promoting its interaction with the phosphorylated Pol II CTD. Furthermore, our data also indicate that Spt6 recruitment to the 3′ ends of transcribed genes requires the Spt6 tSH2 domain but

not Ser2/Ser5 CTD phosphorylation. This requirement of tSH2 domain for Spt6 recruitment at 3′ORFs suggests a role for Tyr1 phosphorylated Pol II CTD.

Spt6 relies on Ser2 phosphorylation for recruitment to the coding regions. Although it was known that Ser2 phosphorylation enhances Spt6 tSH2 domain interaction with the Pol II CTD *in vitro* (25, 26, 52), it was not clear whether this interaction promotes Spt6 recruitment *in vivo* for several reasons. First, Ser2 phosphorylation peaks 1 kb after the TSS (29), whereas Spt6 is recruited near the 5′ORF. Second, deleting Ctk1, the primary Ser2 kinase, did not reduce Spt6 recruitment to the coding regions (Fig. 1B, D, and E) (27). Finally, deleting the tSH2 domain substantially reduced but did not completely abolish Spt6 binding across the ORF (Fig. 7D) (22). All of these observations lead to a suggestion that Spt6 recruitment to the 5′ORF occurs in a phospho CTD-independent manner (22, 52). Our results, however, clearly show that Spt6 recruitment to the coding regions is promoted redundantly by both Ser2 kinases (Bur1 and Ctk1) (Fig. 1). Unexpectedly, these kinases promote recruitment of Spt6 at the 5′ proximal regions (Fig. 2), whereas Ser2 phosphorylation is generally low in that region. These results are consistent with the role of Bur1 and Ctk1 in phosphorylating Ser2 near the 5′ORFs (28, 42) and is analogous to the role of Ser2 phosphorylation in recruiting the Paf1 complex (53), which is also recruited early during the transition from initiating to elongating. Our study makes two important observations regarding the role of Ser2 kinases in Spt6 recruitment. First, although *bur1as* reduced Spt6 recruitment in the 5′ORFs of *ARG1* and *ADH1*, a greater reduction of Spt6 occupancy in the *bur1as/ctk1*Δ mutant indicates the importance of Ctk1 kinase activity for full recruitment during early transcription. Second, unlike the high levels of Ser2P required for recruiting termination/mRNA processing factors near 3′ ends of transcribed genes (27), the low levels of Ser2P at 5′ORF are sufficient to efficiently recruit Spt6. These results are further supported by our ChIP-chip results showing maximum Spt6 binding defects at the 5′ORFs in the *bur1as/ctk1*Δ double mutant (Fig. 2).

In addition to phosphorylating the Pol II CTD on Ser2, Bur1 also phosphorylates the Spt5 C-terminal region (CTR), which consists of 15 hexapeptide repeats (53–55). Considering this, along with the fact that Spt6 interacts with Spt5 (54), it is possible that Bur1 contributes in Spt6 recruitment through Spt5-CTR phosphorylation. However, an earlier study (54) showed that deleting Spt5-CTR did not impair Spt5-Spt6 interaction and, more recently, it was reported that Spt5-CTR did not significantly reduce Spt6 binding *in vivo* (56). Although the role of phospho-CTR in Spt6 recruitment cannot be ruled out, these studies, along with our results, strongly suggest that Bur1, together with Ctk1, promote Spt6 recruitment in a phosphorylated Ser2-dependent manner.

Role of HDACs in Spt6 recruitment. In addition to CTD phosphorylation, we provide evidence that HDACs (Rpd3 and Hos2) regulate Spt6 occupancy in the coding regions. The *rpd3*Δ/*hos2*Δ double mutant reduced Spt6 binding in the ORFs (Fig. 4D and E), and the genome-wide experiments revealed that the maximum defect in Spt6 binding occurs in the middle of transcribed regions (Fig. 4G to I). These regions are enriched for H3K4 and H3K36 dimethylated histones, which are targeted by Hos2-Set3C and Rpd3S complexes for deacetylation (47–49, 51). It is therefore interesting to see that the maximum defect in Spt6 binding is observed in the region of transcribed ORFs where these HDACs deacetylate nucleosomes. Although this suggests that hyperacetylated nucleosomes suppress the association of Spt6 with coding regions in the HDAC mutant, our data suggest a new role for HDACs in regulating Spt6 occupancy apart from deacetylating ORF nucleosomes. In support of this, Spt6 occupancy (Fig. 5B and D), as well as the Spt6-Pol II interaction (Fig. 6A), are retained in the *set1*Δ/*set2*Δ mutant. Since this mutant increases histone acetylation (Fig. 5F to H) (35, 47–49), it appears that hyperacetylated nucleosomes are not sufficient to prevent Spt6 occupancy in *rpd3*Δ/*hos2*Δ cells. Our observation that *rpd3*Δ/*hos2*Δ diminishes Spt6-Pol II interactions (Fig. 5A and 6F) indicates that HDACs promote Spt6 binding to Pol II and thereby reduce Spt6 occupancy in ORFs. Loss of Spt6-Pol II interactions in the *rpd3*Δ/*hos2*Δ mutant is not totally unexpected, considering the fact that both HDACs and Spt6 bind to the phosphorylated Pol II (Fig. 5A) (35). HDACs can thereby promote this interaction. Efficient coimmunoprecipitation of Spt6 with both Rpd3 and Rco1 (Fig. 6E) provides support for these HDACs enhancing Spt6 occupancy in the coding regions. We propose that CTD-bound HDACs (Rpd3 and Hos2) strengthen Spt6 and phospho-Pol II interactions, allowing Spt6 to migrate farther into coding regions. However, this interaction is labile in the absence of HDACs, and results in reduced Spt6 occupancy in TSS-distal regions. This is supported by our results showing that deleting HDACs did not further reduce binding of Spt6 lacking the tSH2 domain (Fig. 7D and E). Whether a physical interaction between Spt6 and HDACs is sufficient to prevent premature dissociation of Spt6 from the transcribed regions or dynamic acetylation of a nonhistone protein(s), perhaps Spt6 itself, plays a role in enhancing Spt6 association with the transcribed regions remains to be elucidated.

Since Rpd3S and Hos2-Set3 are recruited to the phosphorylated Pol II CTD in a manner dependent on Ser5 phosphorylation by Kin28 (35, 51), it was surprising to see that the *kin28as/bur2*Δ mutation did not reduce Spt6 binding. However, drastic reductions in Pol II occupancy, particularly in the middle of coding regions in the *kin28as/bur2*Δ mutant, made it difficult to assess a Spt6 binding defect due to the impaired HDAC recruitment in this mutant.

Minimal coimmunoprecipitation of H3 with Spt6 in the *rpd3*Δ/*hos2*Δ mutant (Fig. 6F) is most likely the result of reduced Spt6 binding in the coding region rather than an inability of Spt6 to recognize or bind histones. This is supported by the fact that both unmodified and acetylated H3 and H4 N-terminal tail peptides pulled down similar amounts of Spt6 from whole-cell extracts (Fig. 6B). However, the reduced histone occupancy in the coding regions in the HDAC mutant (35) might have also contributed in inefficient coimmunoprecipitation of histone H3 with Spt6 in this strain.

Our results also demonstrate the importance of the tSH2 domain in recruiting Spt6 at both ends of the transcription units (Fig. 7D and E). The tSH2 domain relies on Ser2 phosphorylation for recruiting Spt6 near early transcribed regions since Spt6 occupancy is greatly reduced in the 5′ORFs in the *bur1as/ctk1*Δ mutant. However, the inability of the Ser2 kinase mutants to dampen Spt6 recruitment near the 3′ ends indicates that tSH2-mediated Spt6 recruitment toward the end is carried out in a Ser2P-independent manner. Given that the tSH2 binds with greater affinity to the CTD peptides phosphorylated at Tyr1 than at Ser2 or Ser5 and that the Tyr1P peak coincides with the Spt6 binding peak at the 3′ ends (23, 24), our results strongly suggest that Spt6 recruit-

ment toward the 3′ end is mediated through Tyr1P-tSH2 domain interactions.

In conclusion, our study provides *in vivo* evidence for the importance of Ser2 in recruiting Spt6 to the 5′ ends of transcribed genes. As Pol II elongates farther away from the TSS, HDACs prevent premature dissociation of Spt6 from the elongating Pol II. Increasing levels of Tyr1 phosphorylation toward the 3′ end then stabilizes Spt6-Pol II CTD interaction via the tSH2 domain. A recent study showed preferential loss of histones from the 5′ ends of the transcribed genes in Spt6-depleted cells (16). We speculate that Spt6 recruitment by Ser2 phosphorylation is important for regulating histone occupancy near the 5′ ends. Spt6 interaction with HDACs would facilitate association with the mid-ORF region, which may contribute in efficient reassembly of histones displaced in the wake of Pol II elongation, and in preventing cryptic transcription which tends to originate within intragenic regions (15, 19). Finally, Tyr1P-mediated recruitment of Spt6 at the 3′ ends of genes might help in coordinating transcription termination and mRNA processing (57, 58).

ACKNOWLEDGMENTS

We are grateful to Tim Formosa for providing Spt6 antibodies and Joseph Reese for strains deleted for histone deacetylases. We thank Paola Yumpo and Kathleen A. Lesich for critical reading of the manuscript.

This research was supported in part by grants from the National Institutes of Health (GM095514) and the Center of Biomedical Research (Oakland University) to C.K.G. and the Canadian Institutes of Health Research (MOP-133648) to F.R.

REFERENCES

1. **Spain MM, Govind CK.** 2011. A role for phosphorylated Pol II CTD in modulating transcription coupled histone dynamics. Transcription **2:**78–81. http://dx.doi.org/10.4161/trns.2.2.14638.
2. **Li B, Carey M, Workman JL.** 2007. The role of chromatin during transcription. Cell **128:**707–719. http://dx.doi.org/10.1016/j.cell.2007.01.015.
3. **Adkins MW, Tyler JK.** 2006. Transcriptional activators are dispensable for transcription in the absence of Spt6-mediated chromatin reassembly of promoter regions. Mol. Cell **21:**405–416. http://dx.doi.org/10.1016/j.molcel.2005.12.010.
4. **Compagnone-Post PA, Osley MA.** 1996. Mutations in the SPT4, SPT5, and SPT6 genes alter transcription of a subset of histone genes in *Saccharomyces cerevisiae*. Genetics **143:**1543–1554.
5. **Ardehali MB, Yao J, Adelman K, Fuda NJ, Petesch SJ, Webb WW, Lis JT.** 2009. Spt6 enhances the elongation rate of RNA polymerase II in vivo. EMBO J. **28:**1067–1077. http://dx.doi.org/10.1038/emboj.2009.56.
6. **Hartzog GA, Wada T, Handa H, Winston F.** 1998. Evidence that Spt4, Spt5, and Spt6 control transcription elongation by RNA polymerase II in *Saccharomyces cerevisiae*. Genes Dev. **12:**357–369. http://dx.doi.org/10.1101/gad.12.3.357.
7. **Begum NA, Stanlie A, Nakata M, Akiyama H, Honjo T.** 2012. The histone chaperone Spt6 is required for activation-induced cytidine deaminase target determination through H3K4me3 regulation. J. Biol. Chem. **287:**32415–32429. http://dx.doi.org/10.1074/jbc.M112.351569.
8. **Malagon F, Aguilera A.** 2001. Yeast *spt6-140* mutation, affecting chromatin and transcription, preferentially increases recombination in which Rad51p-mediated strand exchange is dispensable. Genetics **158:**597–611.
9. **Andrulis ED, Guzman E, Doring P, Werner J, Lis JT.** 2000. High-resolution localization of *Drosophila* Spt5 and Spt6 at heat shock genes in vivo: roles in promoter proximal pausing and transcription elongation. Genes Dev. **14:**2635–2649. http://dx.doi.org/10.1101/gad.844200.
10. **Cygnar D, Hagemeier S, Kronemann D, Bresnahan WA.** 2012. The cellular protein SPT6 is required for efficient replication of human cytomegalovirus. J. Virol. **86:**2011–2020. http://dx.doi.org/10.1128/JVI.06776-11.
11. **Bortvin A, Winston F.** 1996. Evidence that Spt6p controls chromatin structure by a direct interaction with histones. Science **272:**1473–1476. http://dx.doi.org/10.1126/science.272.5267.1473.
12. **Kato H, Okazaki K, Iida T, Nakayama J, Murakami Y, Urano T.** 2013. Spt6 prevents transcription-coupled loss of posttranslationally modified histone H3. Sci. Rep. **3:**2186. http://dx.doi.org/10.1038/srep02186.
13. **Yoh SM, Cho H, Pickle L, Evans RM, Jones KA.** 2007. The Spt6 SH2 domain binds Ser2-P RNAPII to direct Iws1-dependent mRNA splicing and export. Genes Dev. **21:**160–174. http://dx.doi.org/10.1101/gad.1503107.
14. **Youdell ML, Kizer KO, Kisseleva-Romanova E, Fuchs SM, Duro E, Strahl BD, Mellor J.** 2008. Roles for Ctk1 and Spt6 in regulating the different methylation states of histone H3 lysine 36. Mol. Cell. Biol. **28:**4915–4926. http://dx.doi.org/10.1128/MCB.00001-08.
15. **Ivanovska I, Jacques PE, Rando OJ, Robert F, Winston F.** 2011. Control of chromatin structure by spt6: different consequences in coding and regulatory regions. Mol. Cell. Biol. **31:**531–541. http://dx.doi.org/10.1128/MCB.01068-10.
16. **Perales R, Erickson B, Zhang L, Kim H, Valiquett E, Bentley D.** 2013. Gene promoters dictate histone occupancy within genes. EMBO J. **32:**2645–2656. http://dx.doi.org/10.1038/emboj.2013.194.
17. **Kaplan CD, Laprade L, Winston F.** 2003. Transcription elongation factors repress transcription initiation from cryptic sites. Science **301:**1096–1099. http://dx.doi.org/10.1126/science.1087374.
18. **Cheung V, Chua G, Batada NN, Landry CR, Michnick SW, Hughes TR, Winston F.** 2008. Chromatin- and transcription-related factors repress transcription from within coding regions throughout the *Saccharomyces cerevisiae* Genome. PLoS Biol. **6:**e277. http://dx.doi.org/10.1371/journal.pbio.0060277.
19. **Degennaro CM, Alver BH, Marguerat S, Stepanova E, Davis CP, Bahler J, Park PJ, Winston F.** 2013. Spt6 regulates intragenic and antisense transcription, nucleosome positioning, and histone modifications genome-wide in fission yeast. Mol. Cell. Biol. **33:**4779–4792. http://dx.doi.org/10.1128/MCB.01068-13.
20. **Li B, Gogol M, Carey M, Pattenden SG, Seidel C, Workman JL.** 2007. Infrequently transcribed long genes depend on the Set2/Rpd3S pathway for accurate transcription. Genes Dev. **21:**1422–1430. http://dx.doi.org/10.1101/gad.1539307.
21. **Kim T, Xu Z, Clauder-Münster S, Steinmetz Lars M, Buratowski S.** 2012. Set3 HDAC mediates effects of overlapping noncoding transcription on gene induction kinetics. Cell **150:**1158–1169. http://dx.doi.org/10.1016/j.cell.2012.08.016.
22. **Mayer A, Lidschreiber M, Siebert M, Leike K, Soding J, Cramer P.** 2010. Uniform transitions of the general RNA polymerase II transcription complex. Nat. Struct. Mol. Biol. **17:**1272–1278. http://dx.doi.org/10.1038/nsmb.1903.
23. **Mayer A, Heidemann M, Lidschreiber M, Schreieck A, Sun M, Hintermair C, Kremmer E, Eick D, Cramer P.** 2012. CTD tyrosine phosphorylation impairs termination factor recruitment to RNA polymerase II. Science **336:**1723–1725. http://dx.doi.org/10.1126/science.1219651.
24. **Close D, Johnson SJ, Sdano MA, McDonald SM, Robinson H, Formosa T, Hill CP.** 2011. Crystal structures of the *Saccharomyces cerevisiae* Spt6 core and C-terminal tandem SH2 domain. J. Mol. Biol. **408:**697–713. http://dx.doi.org/10.1016/j.jmb.2011.03.002.
25. **Liu J, Zhang J, Gong Q, Xiong P, Huang H, Wu B, Lu G, Wu J, Shi Y.** 2011. Solution structure of tandem SH2 domains from Spt6 protein and their binding to the phosphorylated RNA polymerase II C-terminal domain. J. Biol. Chem. **286:**29218–29226. http://dx.doi.org/10.1074/jbc.M111.252130.
26. **Diebold ML, Loeliger E, Koch M, Winston F, Cavarelli J, Romier C.** 2010. Noncanonical tandem SH2 enables interaction of elongation factor Spt6 with RNA polymerase II. J. Biol. Chem. **285:**38389–38398. http://dx.doi.org/10.1074/jbc.M110.146696.
27. **Ahn SH, Kim M, Buratowski S.** 2004. Phosphorylation of serine 2 within the RNA polymerase II C-terminal domain couples transcription and 3′ end processing. Mol. Cell **13:**67–76. http://dx.doi.org/10.1016/S1097-2765(03)00492-1.
28. **Qiu H, Hu C, Hinnebusch AG.** 2009. Phosphorylation of the Pol II CTD by KIN28 enhances BUR1/BUR2 recruitment and Ser2 CTD phosphorylation near promoters. Mol. Cell **33:**752–762. http://dx.doi.org/10.1016/j.molcel.2009.02.018.
29. **Bataille AR, Jeronimo C, Jacques PE, Laramee L, Fortin ME, Forest A, Bergeron M, Hanes SD, Robert F.** 2012. A universal RNA polymerase II CTD cycle is orchestrated by complex interplays between kinase, phosphatase, and isomerase enzymes along genes. Mol. Cell **45:**158–170. http://dx.doi.org/10.1016/j.molcel.2011.11.024.
30. **Sharma VM, Tomar RS, Dempsey AE, Reese JC.** 2007. Histone deacety-

lases RPD3 and HOS2 regulate the transcriptional activation of DNA damage-inducible genes. Mol. Cell. Biol. **27:**3199–3210. http://dx.doi.org/10.1128/MCB.02311-06.

31. **Ginsburg DS, Govind CK, Hinnebusch AG.** 2009. NuA4 lysine acetyltransferase Esa1 is targeted to coding regions and stimulates transcription elongation with Gcn5. Mol. Cell. Biol. **29:**6473–6487. http://dx.doi.org/10.1128/MCB.01033-09.
32. **Winzeler EA, Shoemaker DD, Astromoff A, Liang H, Anderson K, Andre B, Bangham R, Benito R, Boeke JD, Bussey H, Chu AM, Connelly C, Davis K, Dietrich F, Dow SW, Bakkoury ME, Foury F, Friend SH, Gentalen E, Giaever G, Hegemann JHJ, Laub TM, Liao H, Liebundguth N, Lockhart DJ, Lucau-Danila A, Lussier M, M'Rabet N, Menard P, Mittmann M, Pai C, Rebischung C, Revuelta JL, Riles L, Roberts CJ, Ross-McDonald P, Scherens B, Snyder M, Sookhai-Mahadeo S, Storms RK, Veronneau S, Voet M, Volckaert G, Ward TR, Wysocki R, Yen GS, Yu K, Zimmermann K, Philippsen P, Johnston M, Davis RW.** 1999. Functional characterization of the *Saccharomyces cerevisiae* genome by gene deletion and parallel analysis. Science **285:**901–906. http://dx.doi.org/10.1126/science.285.5429.901.
33. **Mnaimneh S, Davierwala AP, Haynes J, Moffat J, Peng WT, Zhang W, Yang X, Pootoolal J, Chua G, Lopez A, Trochesset M, Morse D, Krogan NJ, Hiley SL, Li Z, Morris Q, Grigull J, Mitsakakis N, Roberts CJ, Greenblatt JF, Boone C, Kaiser CA, Andrews BJ, Hughes TR.** 2004. Exploration of essential gene functions via titratable promoter alleles. Cell **118:**31–44. http://dx.doi.org/10.1016/j.cell.2004.06.013.
34. **Govind CK, Zhang F, Qiu H, Hofmeyer K, Hinnebusch AG.** 2007. Gcn5 promotes acetylation, eviction, and methylation of nucleosomes in transcribed coding regions. Mol. Cell **25:**31–42. http://dx.doi.org/10.1016/j.molcel.2006.11.020.
35. **Govind CK, Qiu H, Ginsburg DS, Ruan C, Hofmeyer K, Hu C, Swaminathan V, Workman JL, Li B, Hinnebusch AG.** 2010. Phosphorylated Pol II CTD recruits multiple HDACs, including Rpd3C(S), for methylation-dependent deacetylation of ORF nucleosomes. Mol. Cell **39:**234–246. http://dx.doi.org/10.1016/j.molcel.2010.07.003.
36. **Govind CK, Ginsburg D, Hinnebusch AG.** 2012. Measuring dynamic changes in histone modifications and nucleosome density during activated transcription in budding yeast. Methods Mol. Biol. **833:**15–27. http://dx.doi.org/10.1007/978-1-61779-477-3_2.
37. **Ren B, Robert F, Wyrick JJ, Aparicio O, Jennings EG, Simon I, Zeitlinger J, Schreiber J, Hannett N, Kanin E, Volkert TL, Wilson CJ, Bell SP, Young RA.** 2000. Genome-wide location and function of DNA binding proteins. Science **290:**2306–2309. http://dx.doi.org/10.1126/science.290.5500.2306.
38. **Coulombe C, Poitras C, Nordell-Markovits A, Brunelle M, Lavoie MA, Robert F, Jacques PE.** 2014. VAP: a versatile aggregate profiler for efficient genome-wide data representation and discovery. Nucleic Acids Res. **42:**W485–W493. http://dx.doi.org/10.1093/nar/gku302.
39. **Xu Z, Wei W, Gagneur J, Perocchi F, Clauder-Munster S, Camblong J, Guffanti E, Stutz F, Huber W, Steinmetz LM.** 2009. Bidirectional promoters generate pervasive transcription in yeast. Nature **457:**1033–1037. http://dx.doi.org/10.1038/nature07728.
40. **Egloff S, Murphy S.** 2008. Cracking the RNA polymerase II CTD code. Trends Genet. **24:**280–288. http://dx.doi.org/10.1016/j.tig.2008.03.008.
41. **Buratowski S.** 2009. Progression through the RNA polymerase II CTD cycle. Mol. Cell **36:**541–546. http://dx.doi.org/10.1016/j.molcel.2009.10.019.
42. **Liu Y, Warfield L, Zhang C, Luo J, Allen J, Lang WH, Ranish J, Shokat KM, Hahn S.** 2009. Phosphorylation of the transcription elongation factor Spt5 by yeast Bur1 kinase stimulates recruitment of the PAF complex. Mol. Cell. Biol. **29:**4852–4863. http://dx.doi.org/10.1128/MCB.00609-09.
43. **Dronamraju R, Strahl BD.** 2014. A feed forward circuit comprising Spt6, Ctk1, and PAF regulates Pol II CTD phosphorylation and transcription elongation. Nucleic Acids Res. **42:**870–881. http://dx.doi.org/10.1093/nar/gkt1003.
44. **Kim H, Erickson B, Luo W, Seward D, Graber JH, Pollock DD, Megee PC, Bentley DL.** 2010. Gene-specific RNA polymerase II phosphorylation and the CTD code. Nat. Struct. Mol. Biol. **17:**1279–1286. http://dx.doi.org/10.1038/nsmb.1913.
45. **Jeronimo C, Robert F.** 2014. Kin28 regulates the transient association of Mediator with core promoters. Nat. Struct. Mol. Biol. **21:**449–455. http://dx.doi.org/10.1038/nsmb.2810.
46. **Wong KH, Jin Y, Struhl K.** 2014. TFIIH phosphorylation of the Pol II CTD stimulates mediator dissociation from the preinitiation complex and promoter escape. Mol. Cell **54:**601–612. http://dx.doi.org/10.1016/j.molcel.2014.03.024.
47. **Kim T, Buratowski S.** 2009. Dimethylation of H3K4 by Set1 recruits the Set3 histone deacetylase complex to 5′ transcribed regions. Cell **137:**259–272. http://dx.doi.org/10.1016/j.cell.2009.02.045.
48. **Carrozza MJ, Li B, Florens L, Suganuma T, Swanson SK, Lee KK, Shia WJ, Anderson S, Yates J, Washburn MP, Workman JL.** 2005. Histone H3 methylation by Set2 directs deacetylation of coding regions by Rpd3S to suppress spurious intragenic transcription. Cell **123:**581–592. http://dx.doi.org/10.1016/j.cell.2005.10.023.
49. **Keogh MC, Kurdistani SK, Morris SA, Ahn SH, Podolny V, Collins SR, Schuldiner M, Chin K, Punna T, Thompson NJ, Boone C, Emili A, Weissman JS, Hughes TR, Strahl BD, Grunstein M, Greenblatt JF, Buratowski S, Krogan NJ.** 2005. Cotranscriptional set2 methylation of histone H3 lysine 36 recruits a repressive Rpd3 complex. Cell **123:**593–605. http://dx.doi.org/10.1016/j.cell.2005.10.025.
50. **Psathas JN, Zheng S, Tan S, Reese JC.** 2009. Set2-dependent K36 methylation is regulated by novel intratail interactions within H3. Mol. Cell. Biol. **29:**6413–6426. http://dx.doi.org/10.1128/MCB.00876-09.
51. **Drouin S, Laramée L, Jacques P-É, Forest A, Bergeron M, Robert F.** 2010. DSIF and RNA polymerase II CTD phosphorylation coordinate the recruitment of Rpd3S to actively transcribed genes. PLoS Genet. **6:**e1001173. http://dx.doi.org/10.1371/journal.pgen.1001173.
52. **Sun M, Lariviere L, Dengl S, Mayer A, Cramer P.** 2010. A tandem SH2 domain in transcription elongation factor Spt6 binds the phosphorylated RNA polymerase II C-terminal repeat domain (CTD). J. Biol. Chem. **285:**41597–41603. http://dx.doi.org/10.1074/jbc.M110.144568.
53. **Qiu H, Hu C, Gaur NA, Hinnebusch AG.** 2012. Pol II CTD kinases Bur1 and Kin28 promote Spt5 CTR-independent recruitment of Paf1 complex. EMBO J. **31:**3494–3505. http://dx.doi.org/10.1038/emboj.2012.188.
54. **Swanson MS, Winston F.** 1992. SPT4, SPT5, and SPT6 interactions: effects on transcription and viability in *Saccharomyces cerevisiae*. Genetics **132:**325–336.
55. **Zhou K, Kuo WH, Fillingham J, Greenblatt JF.** 2009. Control of transcriptional elongation and cotranscriptional histone modification by the yeast BUR kinase substrate Spt5. Proc. Natl. Acad. Sci. U. S. A. **106:**6956–6961. http://dx.doi.org/10.1073/pnas.0806302106.
56. **Mayer A, Schreieck A, Lidschreiber M, Leike K, Martin DE, Cramer P.** 2012. The spt5 C-terminal region recruits yeast 3′ RNA cleavage factor I. Mol. Cell. Biol. **32:**1321–1331. http://dx.doi.org/10.1128/MCB.06310-11.
57. **Kaplan CD, Holland MJ, Winston F.** 2005. Interaction between transcription elongation factors and mRNA 3′-end formation at the *Saccharomyces cerevisiae GAL10-GAL7* locus. J. Biol. Chem. **280:**913–922. http://dx.doi.org/10.1074/jbc.M411108200.
58. **Bucheli ME, Buratowski S.** 2005. Npl3 is an antagonist of mRNA 3′ end formation by RNA polymerase II. EMBO J. **24:**2150–2160. http://dx.doi.org/10.1038/sj.emboj.7600687.